Natural Variation in Diauxic Shift between Patagonian *Saccharomyces eubayanus* Strains

Jennifer Molinet,[a,b]+ Juan I. Eizaguirre,[c]+ Pablo Quintrel,[a,b] Nicolás Bellora,[d] Carlos A. Villarroel,[a,e,f] Pablo Villarreal,[a,b] José Benavides-Parra,[b] Roberto F. Nespolo,[a,g,h,i] Diego Libkind,[c]# Francisco A. Cubillos[a,b,g]#

[a] ANID-Millennium Science Initiative-Millennium Institute for Integrative Biology (iBio), Santiago, Chile.

[b] Departamento de Biología, Facultad de Química y Biología, Universidad de Santiago de Chile, Santiago, Chile.

[c] Instituto Andino Patagónico de Tecnologías Biológicas y Geoambientales (IPATEC), Universidad Nacional del Comahue, CONICET, CRUB, San Carlos de Bariloche, Río Negro, Argentina.

[d] Instituto de Tecnologías Nucleares para la Salud (INTECNUS), Consejo Nacional de Investigaciones Científicas y Técnicas (CONICET), San Carlos de Bariloche, Argentina.

[e] Instituto de Ciencias Biológicas, Universidad de Talca, Talca, Chile.

[f] Instituto de Investigación Interdisciplinaria (I3), Universidad de Talca, Talca, Chile.

[g] ANID-Millennium Nucleus of Patagonian Limit of Life (LiLi), Valdivia, Chile.

[h] Instituto de Ciencias Ambientales y Evolutivas, Facultad de Ciencias, Universidad Austral de Chile, Valdivia, Chile.

[I] Center of Applied Ecology and Sustainability (CAPES), Santiago, Chile.

+These authors contributed equally to this work.

*Current address: Nicolás Bellora, Instituto de Tecnologías Nucleares para la Salud (INTECNUS), Consejo Nacional de Investigaciones Científicas y Técnicas (CONICET), San Carlos de Bariloche, Argentina.

#Address correspondence to Francisco A. Cubillos, francisco.cubillos.r@usach.cl, and Diego Libkind, libkindfd@comahue-conicet-gob.ar

Running title: Diauxic shift across *S. eubayanus* strains

Abstract (max 250 words)

The study of natural variation can untap novel alleles with immense value for biotechnological applications. *Saccharomyces eubayanus* Patagonian isolates exhibit differences in the diauxic shift between glucose and maltose, representing a suitable model to study their natural genetic variation for novel strains for brewing. However, little is known about the genetic variants and chromatin regulators responsible for these differences. Here, we show how genome-wide chromatin accessibility and gene expression differences underlie distinct diauxic shift profiles in *S. eubayanus*. We identified two strains with a rapid diauxic shift between glucose and maltose (CL467.1 and CBS12357) and one strain with a remarkably low fermentation efficiency and longer lag phase during diauxic shift (QC18). This is associated in the QC18 strain to lower transcriptional activity and chromatin accessibility of specific genes of maltose metabolism, and higher expression levels of glucose transporters. These differences are governed by the HAP complex, which differentially regulates gene expression depending on the genetic background. We found in the QC18 strain a contrasting phenotype to those described in *S. cerevisiae*, where *hap4Δ*, *hap5Δ* and *cin5Δ* knockouts significantly improved the QC18 growth rate in the glucose-maltose shift. The most profound effects were found between *CIN5* allelic variants, suggesting that Cin5p could strongly activate a repressor of the diauxic shift in the QC18 strain, but not necessarily in the other strains. The differences between strains could originate from the tree host from which the strains were obtained, which might determine the sugar source preference and the brewing potential of the strain.

Importance (max 150 words)

The diauxic shift has been studied in the budding yeast under laboratory conditions, however, few studies have addressed the diauxic shift between carbon sources under fermentative conditions. Here, we study the transcriptional and chromatin structure differences that explain the natural variation in fermentative capacity and efficiency during diauxic shift of natural isolates of *S. eubayanus*. Our results show how natural genetic variants in transcription factors impact sugar consumption preferences between strains. These variants have different effects depending on the genetic background, with a contrasting phenotype to those previously described in *S. cerevisiae.* Our study shows how relatively simple genetic/molecular modifications/editing in the lab can facilitate the study of natural variation of microorganisms for the brewing industry.

Keywords: *Saccharomyces eubayanus*, wild strains, beer, RNA-seq, ATAC-seq, diauxic shift, HAP.

INTRODUCTION

The *Saccharomyces cerevisiae* domestication process represents a textbook example of the adaptation of microorganisms to anthropogenic settings (1). However, life in the wild for *Saccharomyces* species is still poorly understood (2). Since the recent discovery and identification of *Saccharomyces eubayanus* (3), one of the parents of the lager yeast hybrid, several studies developed biotechnological applications, together with research studies on its ecology, genetics, evolution, phylogeography and natural history (4–10). *S. eubayanus* isolates have only been found in natural environments; however, the genetic material of *S. eubayanus* has been identified on multiple occasions in industrial hybrids, highlighting the

existence of recurrent hybridization events between *Saccharomyces* species under the human-driven fermentative environment (3, 11–13). Fermentation at low temperatures carried out by the lager hybrid, *Saccharomyces pastorianus*, is undoubtedly the most important of these cases. It is clear then, that *S. eubayanus*, analyzed in both natural and domesticated environments, represents an excellent experimental model for investigating physiological adaptation to both scenarios.

S. pastorianus is a classic example of hybrid vigor. It combines the cold tolerance of *S. eubayanus* together with the superior fermentation kinetics inherited from *S. cerevisiae*, both traits having synergistic effects on fitness, under the cold fermentative environment of European cellars since the middle ages (12, 14, 15). However, despite the importance of *S. pastorianus* in the brewing industry, the origin of this hybrid has not been entirely unraveled (12). This lack of information remains mostly because *S. eubayanus* has never been isolated in Europe, either in fermentation environments or in the wild (16). Paradoxically, this cryotolerant species has been extensively recovered in Argentina (3, 6), North America (17, 18), East Asia (19), New Zealand (20) and Chile (4). Although the evolutionary origin of this species is still a matter of debate, the large number of isolates, lineages and the great genetic diversity found in the Andean region of Argentina and Chile support the hypothesis of a Patagonian origin for *S. eubayanus* (4, 5). This species is genetically structured into two main populations (PA and PB) and 6 subpopulations (HOL, PA-1, PA-2, PB-1, PB-2 and PB-3) (6, 17, 18), reflected in its biogeography (4, 5).

One of the most important parameters to evaluate in brewing fermentation is attenuation, that is, the ability of yeast to consume the sugars from the wort (21). A beer wort is mainly made up of glucose, maltose, maltotriose and dextrins (22). While *S. pastorianus* can consume all

of these sugars, *S. eubayanus* is capable of metabolizing just glucose and maltose, but is unable to consume more complex sugars, such as maltotriose (23). Partial sugar consumption can result in sluggish fermentations, that alter the sensorial properties of the final product (24, 25). Maltose is the most abundant sugar in the wort (approx. 60%) and the efficient consumption of this sugar is decisive in beer fermentation (26). However, the maltose consumption rate in *S. eubayanus* and other *Saccharomyces* species is slower compared to that of commercial lager strains, which are capable of rapidly fermenting all the sugars present in the wort (8, 27, 28). Furthermore, different *S. eubayanus* strains exhibit differences in their maltose consumption rate and yield during fermentation (6, 8). The differences in fermentation rate originate from the phenotypic variation of the metabolic response to the presence of glucose in the medium. This sugar represses the expression of genes involved in the consumption of more complex sugars such as maltose, as well as genes involved in respiration, a phenomenon known as 'glucose repression' (29). Glucose depletion activates a metabolic rewiring triggering the metabolism of other sugars, a process called diauxic shift, which may explain differences in the adaptation time between different *S. eubayanus* strains (30, 31). Then, a detailed molecular analysis of the diauxic shift in *S. eubayanus* strains is fundamental for the potential use of this wild yeast in the industry.

To identify the molecular origin of the variability in sugar consumption at low temperatures between natural *S. eubayanus* yeast strains, we studied the fermentation profiles of 19 strains of *S. eubayanus* that represent the different lineages distributed across Andean Patagonia. Given the great genetic diversity already documented in these lineages and the phenotypic changes observed in previous studies, we selected three strains from Patagonia to evaluate gene expression and chromatin structure differences in depth during the diauxic shift. This

119 approach offered valuable information on the genetic variants underlying sugar consumption
120 differences during fermentation, providing important insights into the ecology of the species,
121 and their potential application in the brewing industry.

122 **RESULTS**

123 ***S. eubayanus* Patagonian isolates exhibit differences in their fermentation profiles**

124 To determine the natural genetic variation in fermentative capacity under brewing conditions
125 across Andean Patagonia *S. eubayanus* isolates, we initially selected 19 strains that are
126 representative of the different geographic areas of Chile and Argentina (**Fig. 1A**, **Table S1A**).
127 After 14 days of beer fermentation, most strains exhibited similar kinetic profiles of CO_2
128 loss, except for the QC18 strain which exhibited the lowest fermentative capacity (**Fig. 1B**,
129 *p-value* < 0.05, Student t-test, **Table S2A, S2B**). Sugar consumption and ethanol production
130 differed across strains (**Table S2C, S2D, S2E**). Interestingly, we observed lower levels of
131 residual maltose and therefore incomplete fermentation, in seven strains (CL204.3, CL211.3,
132 CL215.1, CL218.1, CL444.4, CRUB2031 and CRUB 2108), where the QC18 strain
133 exhibited the lowest consumption levels (ANOVA, *p-value* < 0.0001). However, we did not
134 observe a correlation between residual maltose and CO_2 loss rate (Pearson correlation
135 coefficient -0.33, *p-value* = 0.14, **Fig. S1A**) or maximum CO_2 loss (Pearson correlation
136 coefficient -0.14, *p-value* = 0.54, **Fig. S1A**), likely because residual maltose was below 5
137 g/L. Instead, we found a significant correlation with ethanol production (Pearson correlation
138 coefficient -0.59, *p-value* = 0.005, **Fig. S1A**). Notably, the strains differed in their amino acid
139 consumption profiles at the end of the fermentation, demonstrating differences in their sugar
140 and nitrogen consumption profiles (**Table S2F, S2G, S2H**).

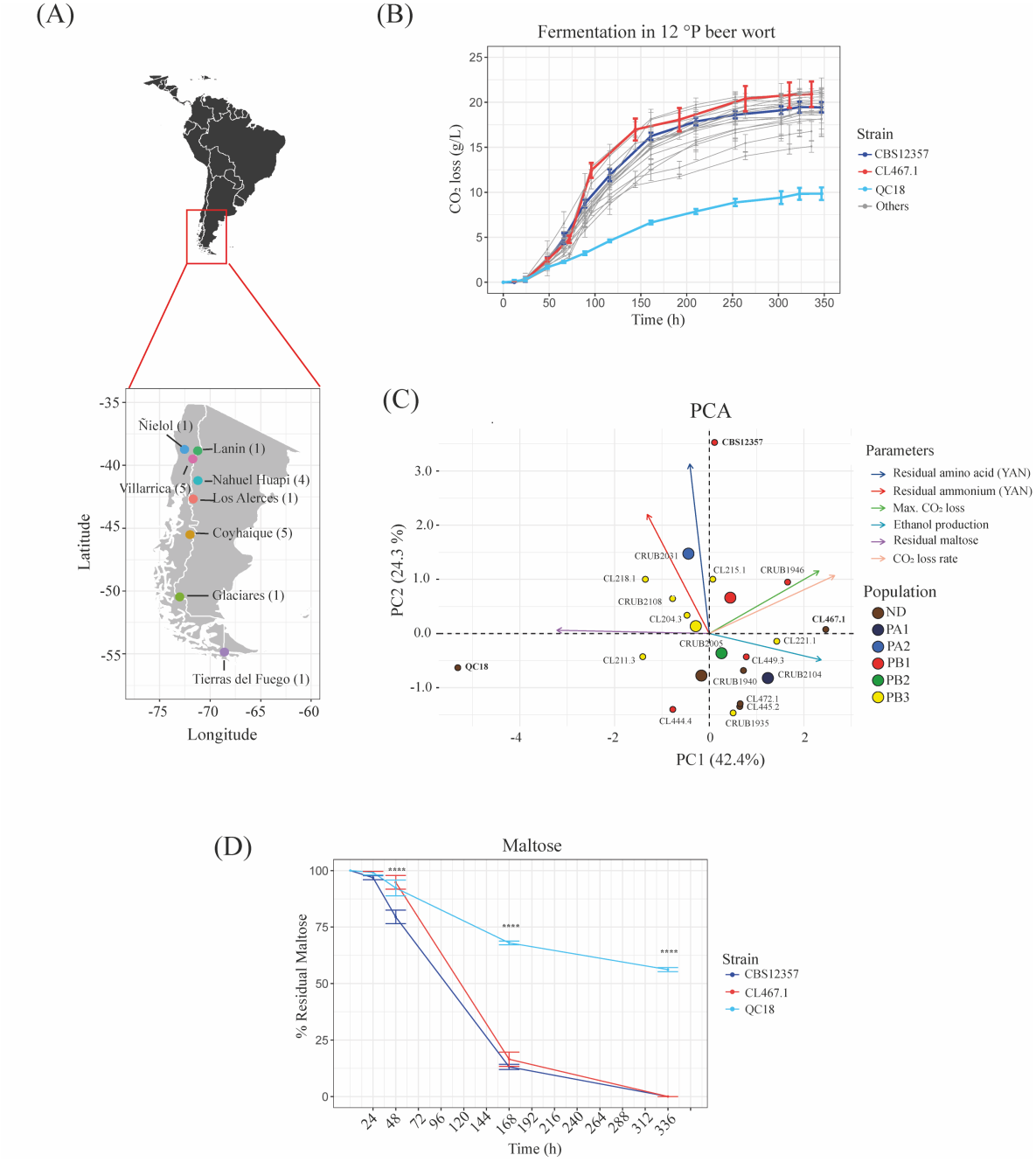

141

142 **Figure 1. Fermentation differences between Andean Patagonia *S. eubayanus* strains.**
143 (A) Map of Argentinian/Chilean Andean Patagonia together with the eight localities from
144 where the 19 strains were isolated. (B) CO_2 loss kinetics for 19 strains; red, blue and light
145 blue depict the three strains selected for the rest of this study. (C) Principal component
146 analysis (PCA) using fermentation parameters across the 19 strains, together with the
147 distribution of individual strains. Arrows depict the different parameters. (D) Maltose
148 consumption kinetics of CBS12357, CL467.1 and QC18 strains. Plotted values correspond
149 to mean values of three independent replicates for each strain. The (*) represents different
150 levels of significance between QC18 and the other strains (t-test, **** $p \leq 0.0001$).

PCA of six fermentation parameters (**Fig. 1C**) indicated that CO_2 loss rate and maximum CO_2 loss parameters correlate positively (Pearson correlation coefficient 0.56, *p-value* = $7.3x10^{-6}$, **Fig. S1B**), where the PC1 and PC2 components explain 42.4% and 24.3% of the observed variance, respectively. Interestingly, the individual factor map indicates no significant separation pattern according to geographical origin and/or phylogenetic group. In addition, we performed hierarchical clustering of the kinetic parameters, obtaining five main clusters (**Fig. S1C**). Again, we did not observe a significant pattern of divergence either by geographic origin or phylogenetic group.

To further explore potential differences between strains throughout the fermentation process, we selected three strains representative of the different phenotypes analyzed above. Of the 19 initial strains, the QC18 strain exhibited the worst kinetic parameters and was selected as a low-fermentation strain (LF). On the other hand, we selected strains CBS12357 and CL467.1 as representatives with higher fermentation capacities (HF). We evaluated the sugar consumption and ethanol production profiles of these three strains at different time-points during the fermentation process (24, 48, 168 and 336 hours, **Table S2C**). Glucose and fructose were completely consumed during the first 48 hours of fermentation independent of the genetic background, while maltose was consumed after 168 hours in the HF strains. However, the LF strain stacked after 48 hours (following glucose/fructose consumption), and we detected maltose consumption after 168 hours (7 days). Overall, the LF strain consumed less than 50% of the maltose after 336 hours, resulting in reduced fermentation capacity and ethanol production (**Fig. 1D**, **Table S2C**).

Similarly, we estimated the yeast assimilable nitrogen consumption (YAN) for the HF and LF strains at different time-points during the fermentation process (24, 48 and 336 hours,

Table S2H). YAN was almost completely consumed after only 48 hours; the CBS12357 strain had slower consumption kinetics compared with the QC18 and CL467.1 strains, mainly for ammonium (Student t-test, *p-value* < 0.0001) and some amino acids during the first 24 hours (alanine, *p-value* < 0.0001, phenylalanine, *p-value* = 0.0484, and leucine, *p-value* = 0.0095, Student t-test, **Table S2H**), and for total YAN amino acids at 48 and 336 hours (Student t-test, *p-value* = 0.0076 and <0.0001, respectively). These results demonstrate that beer fermentation differences across *S. eubayanus* strains are not due to differences in nitrogen consumption, but rather in maltose consumption.

Differences in the glucose-maltose shift between *S. eubayanus* strains

To evaluate the diauxic shift capacity of the HF and LF strains, particularly in the switch from consumption of glucose to other saccharides, we estimated their growth capacity under glucose, maltose, galactose and sucrose after two 24 h pre-cultures in 5% glucose (**Fig. 2**, **Fig. S2** and **Table S3**). In glucose (without diauxic shift), the growth kinetics profiles were similar between strains, yet the lag phase was shorter in the LF strain (Student t-test, *p-value* = 3.9×10^{-7}, **Fig. 2A**). In contrast, we observed a significant difference between the QC18 and HF strains in their growth rates during the glucose-maltose shift (Student t-test, *p-value* = 6×10^{-9}, **Fig. 2B**). This difference was only found for the diauxic shift between glucose-maltose; no differences were observed during the glucose-galactose, or glucose-sucrose transitions (**Fig. S2**) The QC18 strain showed the largest glucose-maltose growth decrease, with a 94% decrease in growth rate and an 89% increase in the duration of the lag phase, compared to HF strains, which exhibited a 31% and 50% decrease in growth rate and a 17% and 22% increase in lag phase duration for the CBS12357 and CL467.1 strains, respectively. When a similar experiment was performed in maltose-maltose conditions, we found lower

differences compared to the glucose-maltose shift, with a decrease in 31% for growth rate, and an increase of 41% for lag phase in the LF strain, while the HF strains exhibited almost no differences in growth rates compared to the glucose-glucose condition (**Fig. 2C**). These results demonstrate that the differences in the glucose-maltose diauxic shift are responsible for the contrasting fermentation profiles between strains.

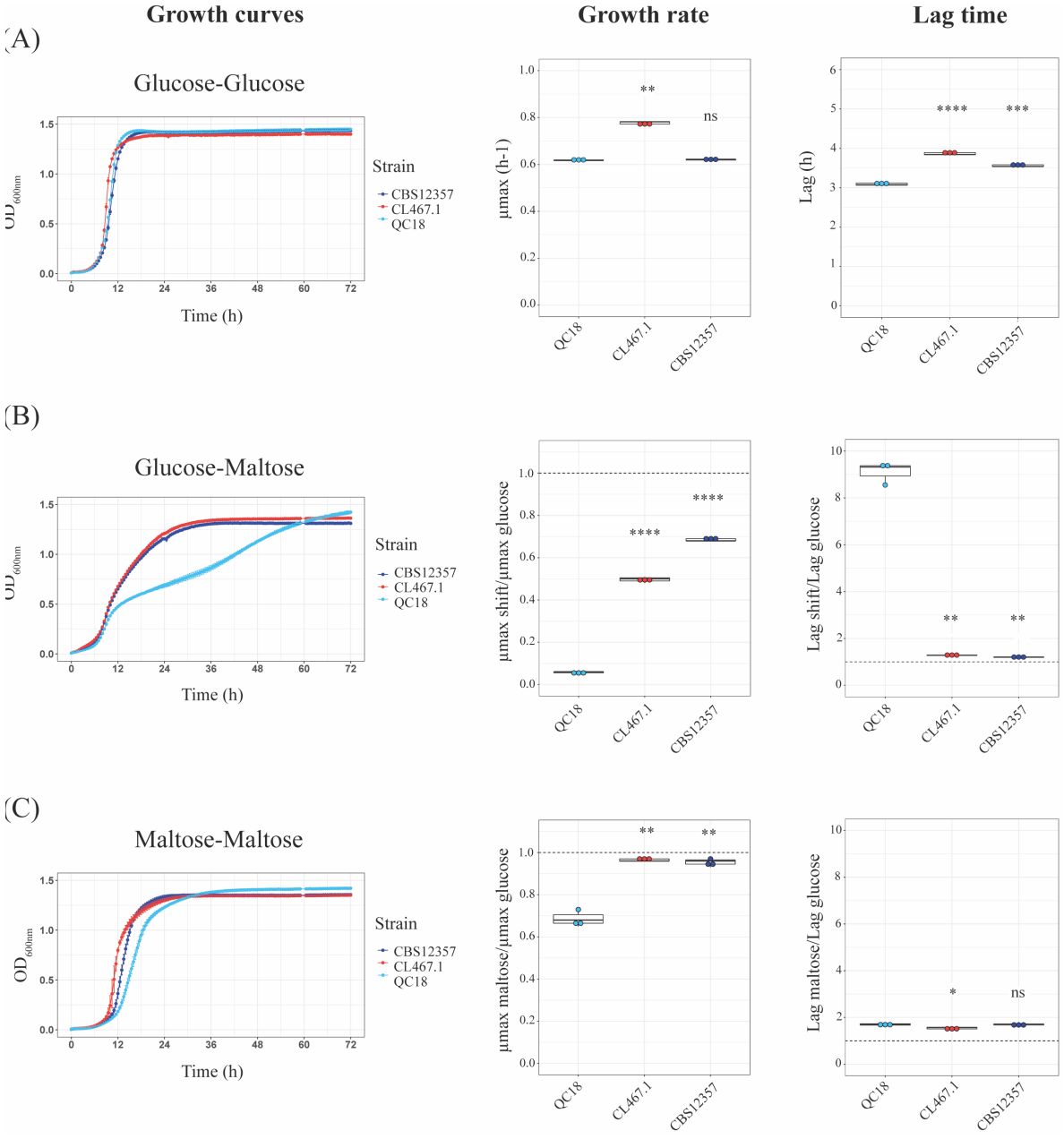

Figure 2. Diauxic shift differences between LF and HF strains during the glucose-maltose shift. (A) Growth curves in glucose and the kinetic parameters: growth rate and lag time. (B) Growth curves in glucose-maltose shifts and the kinetic parameters relative to growth in glucose. (C) Growth curves in maltose and the kinetic parameters relative to the growth in glucose. Plotted values correspond to the mean value of three independent replicates for each strain. The (*) represents different levels of significance between QC18 (LF) and the other strains (CBS12357 and CL467.1, HF) (t-test, * $p \leq 0.05$, ** $p \leq 0.01$, *** $p \leq 0.001$, **** $p \leq 0.0001$).

Comparative transcriptomic analysis reveals transcription factors underlying fermentation differences between strains

To explore global gene expression patterns that could explain fermentation differences between HF and LF strains, we performed RNA-seq analysis on samples collected 24 h after the beginning of the fermentation. We identified 418, 221 and 376 DEGs between CBS12357 vs. QC18, CL467.1 vs. QC18, and CL467.1 vs. CBS12357, respectively (adjusted *p-value* < 0.01 and an absolute value of fold change > 2, **Fig. 3A**, **Table S4A**). We identified a set of 93 DEGs in common between HF vs. the LF strain, which could be related to differences in fermentation capacity. Using hierarchical clustering between HF strains versus the QC18 strain, we identified six clusters of expression profiles **(Fig. 3B**, **Table S4B**).

(A)

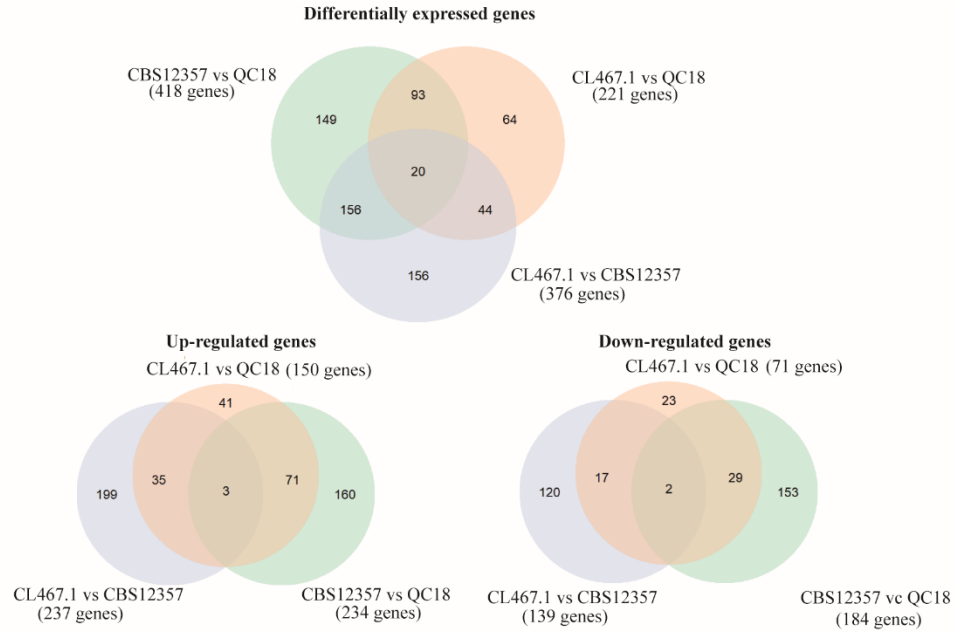

(B)

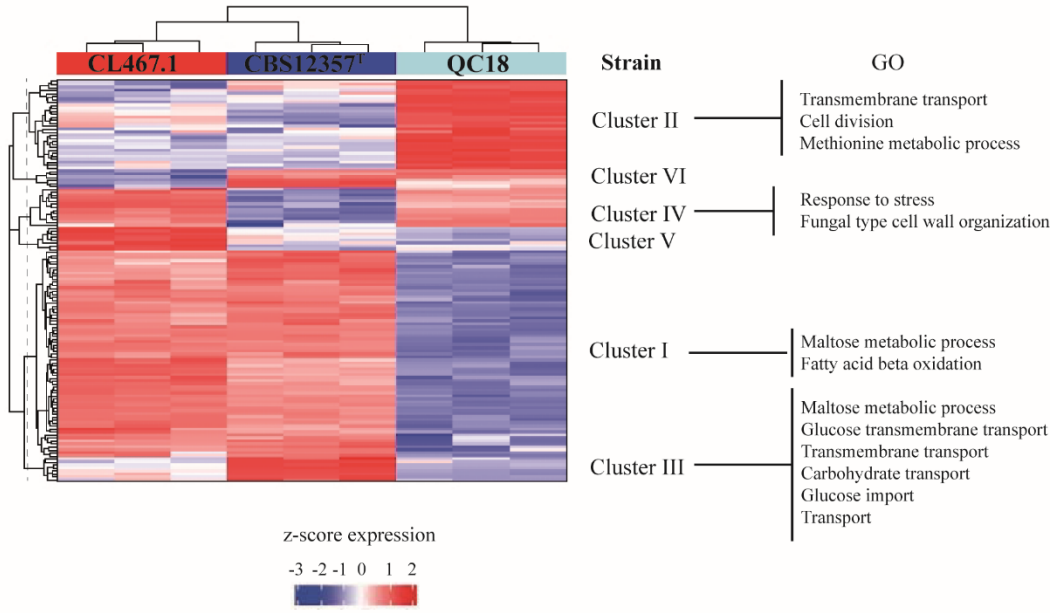

(C)

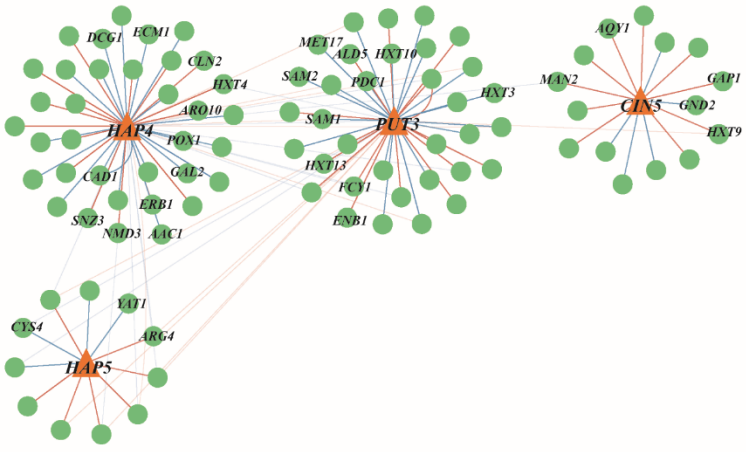

Figure 3. Comparative transcriptome analysis between HF and LF strains. (A) Venn diagram of differentially expressed genes (DEGs), and up and downregulated genes in CBS12357 (HF) vs. QC18 (LF), CL467.1 (HF) vs. QC18 and CL467.1 vs. CBS12357 strains. (B) Hierarchical clustering of DEGs in the three strains. The heatmap was generated using the z-score of expression levels in each comparison. Each row represents a given gene and each column represents a different strain. Clusters are annotated at the right, together with their gene ontology (GO) category. (C) Network analysis of DEGs regulated by Hap4p, Put3p, Cin5p and Hap5 in strains with high fermentation capacity vs. QC18 strain, depicting in bold the most relevant hubs. Red and blue lines represent positive and negative correlations, respectively.

Interestingly, cluster I contained genes related to maltose metabolism and fatty acid beta oxidation, such as *MAL31*, *MAL32*, *IMA1*, *DCI1*, *FOX2* and *PXA2* (**Table S4B, S4C**), which were upregulated in both HF strains. Cluster II contained upregulated genes in the QC18 strains related to transmembrane transport (*HXT5, QDR2* and *ZRT1*), cell division (*CDC6* and *CLN2*) and methionine metabolic processes (*MET10, MET17, SAM2* and *SAM3*). Clusters III to VI showed different expression profile patterns, with differences of expression between both HF strains CBS12357 and CL467.1. We also performed a PCA of DEGs to analyze the expression patterns across the three strains (**Fig. S3A**), where the PC1 and PC2 components explain 62% and 35% of the observed variance, together accounting for 97% of the overall variation. PCA showed a separation of the three strains in both components; the first component separated the CBS12357 strain from the other two strains, while the second component separated the CL467.1 strain from the other two strains. Although HF strains exhibited similar CO_2 loss profiles during the fermentation process, cluster analysis suggests different molecular responses in beer wort across all strains.

We then searched the YeTFaSco database to predict which TFs potentially regulate DEGs (32). We found 76 TFs regulating DEGs between CBS12357 and QC18 (**Table S4D**), 43 TFs regulating DEGs between CL461.1 and QC18 (**Table S4E**), and 129 TFs regulating DEGs between CL467.1 and CBS12357 (**Table S4F**). In order to further investigate the

fermentative differences between the three strains, we selected four TFs enriched related to the diauxic shift and stress responses during fermentation: Hap4p, Hap5, Put3p and Cin5p. TFs belonging to the Hap complex (Hap2p, Hap3p, Hap4p and Hap5p), a global regulator of respiratory gene expression and involved in diauxic shifts (33), were identified in the three comparisons, where Hap5p and Hap4p contain DNA-binding and DNA-activation domains, respectively (33). In addition, Cin5p is a member of the YAP family related to salt and osmotic tolerance (34), while Put3p regulates proline utilization genes (35); both TFs were identified in the comparisons of the two different set of strains. An interaction network analysis for these 4 TFs (**Fig. 3C)** highlighted DEGs in common between HF strains versus QC18, pinpointing genes related to respiration (*AAC1, ATP1, ALD5, YAT1*), nitrogen metabolism (*ARO10, DCG1, SNZ3, FCY1, MET17, SAM1, SAM2, GAP1, ARG4, CYS4*), iron metabolism (*CAD1, ENB1*), cell cycle (*CLN2*), translation (*ECM1, ERB1, NMD3*), hexose transport (*GAL2, HXT4, HXT10, HXT13, HXT3, HXT9*) and fatty acid metabolism (*POX1*).

The four TFs harbor non-synonymous SNPs, with 5, 2, 0 and 2 mutations for *CIN5, HAP4, HAP5* and *PUT3* (**Table S4G**), respectively. However, none of the amino acid substitutions were identified as deleterious to protein function (**Table S4H**). These results suggest that differences in expression levels can likely be explained by differences in polymorphisms within the regulatory regions of the target genes.

Differences in chromatin accessibility and transcription factor binding between *S. eubayanus* strains

We obtained transcription factor binding profiles in all three strains by performing ATAC-seq and measuring chromatin accessibility at promoters. Samples for ATAC-seq were

collected after 20 and 72 h of wort fermentation. Firstly, we analyzed differences in chromatin accessibility at 20 h and compared these to our gene expression results. We found 75 promoters that exhibited differential accessibility among strains (FDR < 0.1) (**Table S4I, S4J**). We analyzed these differences using hierarchical clustering and identified 4 Clusters (**Fig 4A**). The largest cluster (Cluster I) contained promoters showing higher accessibility in HF strains, and low accessibility in QC18. For example, the QC18 strain had lower accessibility and gene expression levels for the hexose transporter (*HXT9*), an activating protein of *CIN4* (*CIN2*), an iso-maltase (*IMA1*) and *GPB1*, a regulator of cAMP-PKA signaling which is involved in the glucose mediated signaling pathway. In addition, in Cluster II, which grouped promoters showing higher accessibility in CBS12357, we found *MAL31* and *MAL32*, suggesting that the higher expression of these genes in CBS12357 could relate to their chromatin configuration. Furthermore, another copy of *MAL32* possessed higher accessibility in QC18, despite showing lower expression in this strain, likely suggesting a role for transcriptional repressors regulating *MAL32* expression in QC18.

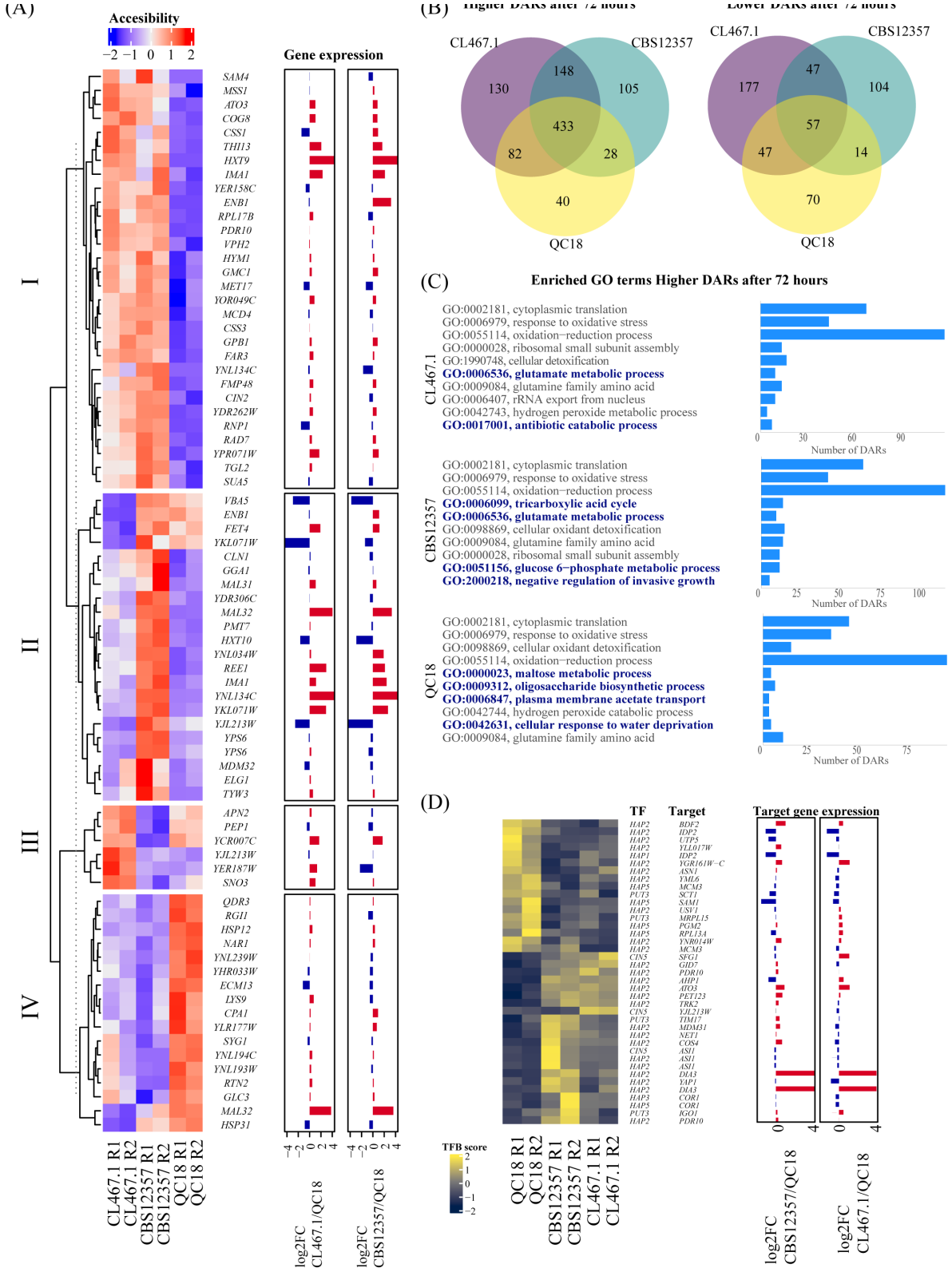

Figure 4. Differences in chromatin accessibility and transcription factor binding between HF and LF strains. (A) The heatmap shows a hierarchical clustering analysis of

chromatin accessibility at promoter regions of HF (CBS12357 and CL467.1) and LF (QC18) strains 20 h after fermentation. Accessibility from ATAC-seq FPKM values were transformed to z-scores and normalized by row. Gene expression at 20 h is shown as log2 fold changes of CL467.1 and CBS12357 relative to QC18. (B) The Venn diagram shows the number of differentially accessible regions (DARs) and their intersection showing higher or lower accessibility in the HF and LF strains in the contrast between 72 and 20 h of fermentation. (C) Gene ontology (GO) enrichment analyses for DARs highlight higher accessibility after 72 h of fermentation. GO terms correspond to Biological Processes. (D) The heatmap shows transcription factor binding scores (TFBS) obtained from ATAC-seq TF binding footprints transformed to z-scores and normalized by row. Gene expression is shown as in (A).

To increase our understanding of the regulatory differences occurring between these strains after the glucose to maltose shift, we analyzed chromatin accessibility differences after 72 h of fermentation. We found across all strains a total of 966 and 516 promoters with increased or decreased accessibility, respectively, when contrasting 72 to 20 h of fermentation (FDR < 0.05). By comparing the sets of differentially accessible regions (DARs) between strains, we found that HF strains shared more DARs that increased accessibility after 72 h than with the LF strain (**Fig. 4B**). Gene ontology analyses of DARs with higher accessibility after 72 h highlighted similarities and differences between strains, where processes such as cytoplasmic translation and oxidative stress responses had increased accessibility in all strains (**Fig. 4C**). In contrast, processes that differed between strains included glutamate metabolism, which was more accessible in HF strains, and maltose metabolism which was more accessible in the LF strain (**Fig. 4C**). These results likely suggest a delayed response in maltose consumption in the LF strain, compared to the HF strains.

Next, by profiling transcription factor binding footprints from ATAC-seq data, we explored the Hap complex, together with Cin5p, and Putp3 binding differences among strains. When examining genome-wide overall transcription factor binding scores (TFBS), we did not find

318 significant differences between strains at 20 or at 72 h of fermentation (**Fig. S3B**), suggesting
319 that these TFs showed similar overall activity among strains. In addition, all differentially
320 bound *Cin5p* binding sites (n=3) showed higher TFBS in HF strains when compared with
321 QC18, with one of these sites associated with lower gene expression in the QC18 strain for
322 *SFG1*, a putative transcription factor involved in the regulation of the mitotic cell cycle (36)
323 (**Fig. 4D**). Interestingly, when dissecting TFBS variation at promoters, we found differences
324 between strains mostly at Hap binding sites, with 25 differentially bound sites for Hap2p
325 (**Fig. 4D**). Among others, we found lower expression levels and greater TFBS in QC18 for
326 *IDP2*, a cytosolic NADP-specific isocitrate dehydrogenase with low levels in the presence
327 of glucose (37), and *SAM1*, an S-adenosylmethionine synthetase which promotes efficient
328 fermentation (38). Overall, these results demonstrate how chromatin accessibility and TFBS
329 differences promote significant differences between strains during the first stages of the beer
330 fermentation process, which impact the fermentative and sugar consumption profile of the
331 strains.

332 ***HAP4*, *HAP5* and *CIN5* impact the diauxic shift capacity in the LF strain**

333 In order to evaluate the effect of Hap4p, Hap5p, Cin5p and Put3p on the diauxic shift and
334 fermentation capacity in the LF and HF strains, we generated null mutants for these four TFs
335 using CRISPR-Cas9 methodology (**Fig. 5A**, **Fig. S4A, S4B, S4C** and **Table S5A**). In HF
336 strains, the *hap4Δ, hap5Δ* and *cin5Δ* knockouts showed a lengthening of the lag phase and
337 an increase in their growth rate after the glucose-maltose shift. In contrast, these knockouts
338 in the QC18 strain exerted a different effect by decreasing the duration of the lag phase and
339 increasing the growth rate, with the greatest effect observed in the *cin5Δ* knockout (~14-fold

increase in growth rate vs. the wild type strain; Student t-test, *p-value* = 3.045×10^{-8}). These results suggest that Cin5p could strongly activate a repressor of the diauxic shift in the LF strain, but not necessarily in the HF strains.

Since *cin5Δ* and *hap5Δ* mutants exerted the strongest phenotypes, we generated double mutants for *cin5Δ/hap5* combinations. Interestingly, in the QC18 strain, the *cin5Δ/hap5* double mutant did not exhibit any differences in terms of lag phase duration, and it possessed a growth rate value between that of the *cin5Δ* and the *hap5* single mutant strains. The equivalent double mutants in the HF strains exhibited a decrease in the lag duration (Student t-test, *p-value* = 0.02117 and 7.1×10^{-6} for CBS12357 and CL467.1 strains, respectively) and a mild increase in their growth rate (Student t-test, *p-value* = 1.6×10^{-4} and 6.8×10^{-6} for CBS12357 and CL467.1 strains, respectively), relative to the wild type strains. For the *put3Δ* null mutants, statistically significant differences were observed solely for the QC18 and CL467.1 strains, with decreases and increases in the duration of the lag phase, respectively (**Fig. 5A**, upper panel), while no differences were observed for growth rate.

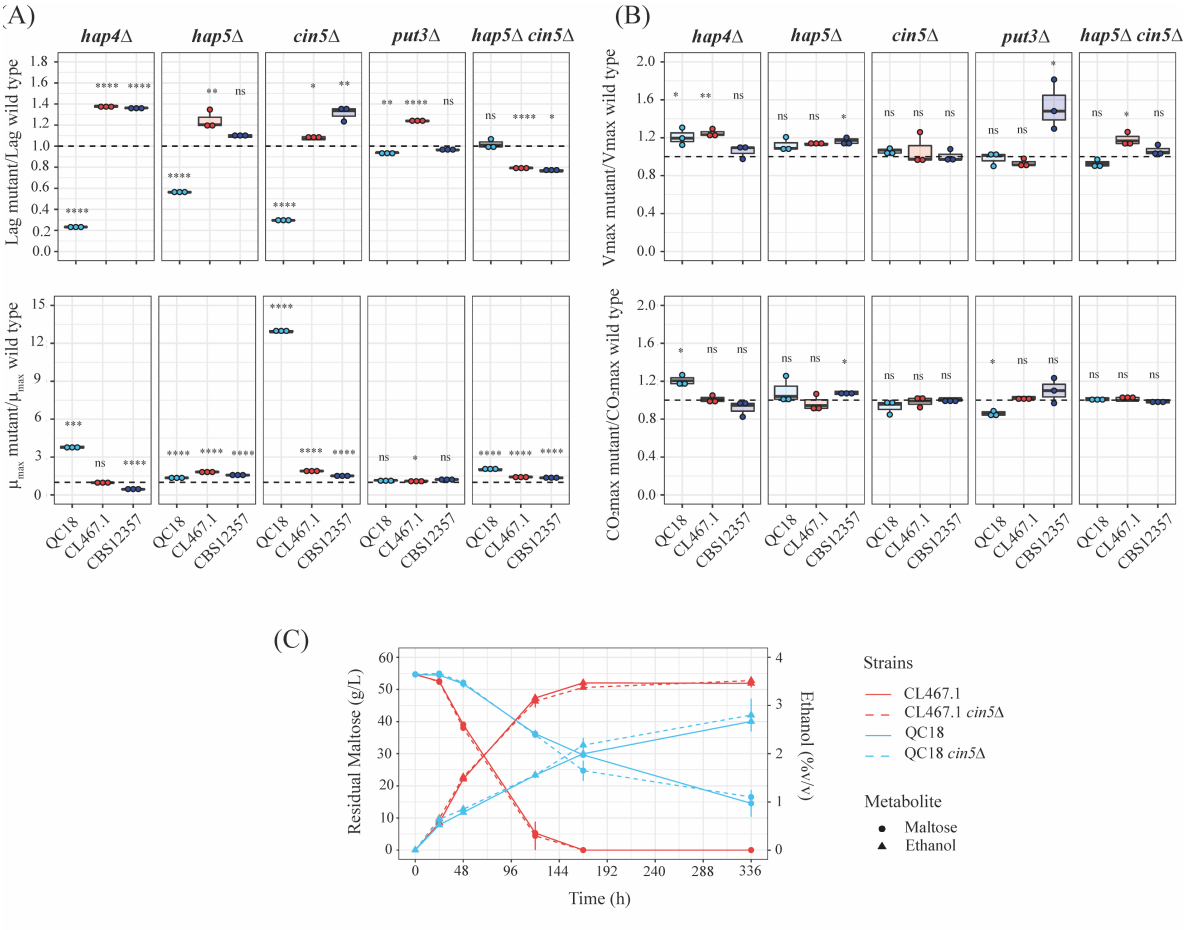

Figure 5. Effect of Hap4p, Hap5, Cin5p and Put3p on diauxic shift and fermentation capacity. (A) Lag time and growth rate of null mutant strains relative to wild type strains after glucose-maltose shift. (B) Fermentation rate and maximum CO_2 loss of null mutant strains relative to wild type strains. (C) Maltose consumption and ethanol production kinetics of CL467.1 and QC18 *cin5Δ* null mutant strains. Plotted values correspond to the means of three independent replicates of each strain. The (*) represents different levels of significance between mutant and wild type strains (t-test, * $p \leq 0.05$, ** $p \leq 0.01$, *** $p \leq 0.001$, **** $p \leq 0.0001$).

We evaluated the effect of mutating these four TFs on the diauxic shift for other sugar sources, such as glucose-galactose and glucose-sucrose (**Fig. S4B, S4C**). In these cases, no differences in the lag phase duration for QC18 mutants after the glucose-galactose shift were observed, except for the double mutant that suffered an increase (Student t-test, *p-value* = 0.0003, **Fig. S4B** upper panels). Furthermore, we detected a rise in the growth rate in almost

all mutants (**Fig. S4B**, lower panels). The glucose-sucrose shift exerted a different pattern. Here, we noted an increase in the lag phase duration and a decrease in the growth rate for the *cin5Δ* and *hap5* QC18 mutants. The four TFs also impacted the fermentation capacity in the three strains under study (**Fig. 5B**, **Table S5B**). Knockout of *HAP4* affected the CO_2 loss rate in QC18 and CL467.1 strains, and the maximum CO_2 loss in the QC18 strain, increasing the fermentation capacity in comparison with their respective wild type strains. A similar effect was observed in the *hap5Δ* knockout of the CBS12357 strain. These results suggest that the TFs Hap4p, Hap5p and Cin5p participate in the diauxic shift between different carbon sources in *S. eubayanus*, but their effect is dependent on the genetic background and the disaccharide carbon source.

To increase our understating of the allelic differences between the three strains during the diauxic shift, we determined the effect of *HAP5* and *CIN5* allelic variants, the two TFs with the greatest effects, by performing a reciprocal hemizygosity analysis between the QC18 and the HF strains (**Fig. S4D**, **Table S5C**). In this assay, we only observed differences between the *CIN5* hemizygous strains, where the *CIN5*-QC18 allele had a lower growth rate compared to the CL467.1 allele (**Fig. S4D**), and a greater lag phase when compared to the CBS12357 allele (**Fig. S4D**), demonstrating a significant effect depending on the *CIN5* allelic version. Finally, we evaluated the kinetics of maltose consumption in *CIN5* null mutants of strains CL467.1 and QC18 under fermentative conditions. Although, we did not observe statistically significant differences during fermentation, the null mutant in QC18 showed a mild tendency to higher maltose consumption after 120 hours (Student t-test, *p-value* = 0.05, **Fig. 5C**, **Table S5D**). Altogether, our results demonstrate that Cin5p significantly affects the glucose-maltose shift in *S. eubayanus* and is dependent on the genetic background.

DISCUSSION

The study of natural variation can identify novel alleles with immense value for the development of novel genetic stocks with applications in several fields. New alleles identified in yeast can improve the fermentation performance of lager hybrids, and the generation of unique fermentative profiles in brewing. Until now, *S. eubayanus* has only been isolated from wild environments and has never been associated with anthropogenic niches. Still, *S. eubayanus* can grow and ferment malt extract, and has a broad phenotypic diversity in terms of fermentative capacities and aroma compound production (4, 6–8, 39). Considering that Patagonian isolates have a greater global genetic diversity, known so far, than Holarctic and Chinese isolates (4, 5), these strains from the southern hemisphere are a rich genetic reservoir for the identification of allelic variants and genetic stocks for the generation of novel hybrids with brewing potential.

Most of the *S. eubayanus* isolates analyzed from Patagonia showed similar fermentation capacities when comparing the maximum CO_2 loss (yield). However, we identified a greater variability in the maximum CO_2 loss rate, mostly due to differences in maltose consumption. Indeed, fermentation rates are of major importance during alcoholic fermentation, mostly because strains able to rapidly ferment all the available sugars can take over the culture and inhibit growth of other microorganisms (24, 40). Glucose promotes catabolite repression, such that maltose uptake usually begins only after half of the initial glucose concentration has been consumed (41). The sensitivity to glucose-induced inhibition is strain specific and the expression of genes responsible for maltose metabolism may be either induced or constitutive (41). Indeed, we found differences between strains in their ability to switch from glucose to maltose, and one of the strains was extremely slow in this transition (LF, QC18).

Studies of wine fermentation have demonstrated that the slow fermentation of fructose is strain- and time-dependent (42). Similarly, the maltose consumption rate of yeast determines the fate of the brewing fermentation process, which differs across strains (43). Thus, consumption rate and residual maltose are of crucial relevance to the brewing industry.

The QC18 strain has the lowest maximum CO_2 loss and CO_2 loss rate values. This strain belong to the PA cluster, and was obtained in the Nahual Huapi National Park (Argentina), but unlike the other strains, QC18 was isolated from the bark of an exotic tree in Patagonia: *Quercus robur* (European oak) (6). Oaks are dominant woody species throughout the northern hemisphere (44), unlike trees belonging to *Nothofagus* genus, which usually form the core of the South Hemisphere primary native forests of Argentina, Chile, Australia and New Zealand (45). The tree-host could determine the phenotypic differences between strains, likely due to differences in the complexity of the available sugars in the bark. In this sense, *Quercus* barks are mostly composed of polysaccharides such as glucose and xylose (46), while *Nothofagus pumilio* trees have higher concentrations of more complex sugar sources, such as starch (47). The QC18 strain has a poor capacity to switch from glucose to maltose, with a decrease in growth rate and an increase in lag time, compared to growth in glucose. There are undoubtedly several factors that may affect the adaptation of the QC18 strain to maltose. During the diauxic shift, there is reduced respiratory activity that lengthens the lag phase, while an over-activation of respiration results in shorter lag phases (25, 48). Upon the sudden loss of glucose, cells enter an energy-deficient state because they are not able to metabolize maltose (48). This energy-deficient state would be exacerbated by decreased respiratory activity in response to glucose. Finally, this state likely prevents induction of *MAL* and subsequent escape from the lag phase. Interestingly, we observed a higher accessibility

437 and higher gene expression levels in *MAL31* and *MAL32* in the CBS12357 strain compared
438 to QC18, suggesting a reduced maltose activity in the latter strain. This reduced adaptation
439 to the diauxic shift was only observed during the shift from glucose to maltose, but not to
440 sucrose or galactose. In agreement with these results, previous studies have demonstrated
441 large differences between strains in gene expression changes and growth rates under different
442 carbon sources, where the diauxic shift depends on both the yeast strain and the carbon source
443 (48, 49).

444 Many genes are influenced by carbon catabolite de-repression during industrial brewery
445 fermentations (50). Analysis of gene expression patterns across strains allowed us to identify
446 strain-dependent mechanisms that explain the differences and similarities in fermentation
447 profiles. In particular, the CBS12357 strain exhibited greater accessibility in the promoter
448 region of the *MAL* genes after 20 hours, whereas the QC18 strain showed lower
449 transcriptional activity of maltose metabolism genes and higher expression levels of *HXT5*,
450 which encodes a functional hexose transporter with a moderate affinity for glucose (51). This
451 gene is regulated by growth rates rather than by extracellular glucose, particularly under
452 conditions that cause slow cell growth, e.g. upon carbon and nitrogen starvation. *HXT5*
453 transcription depends on two HAP complex binding elements, and one post-diauxic shift
454 element in its promoter region (52). The HAP complex (Hap2/3/4/5) plays a central role in
455 converting cells from fermentative to respiratory growth following the diauxic shift by
456 inducing genes required for mitochondrial function upon glucose depletion (25, 48, 53). In
457 this sense, our gene expression analysis identified four TFs that are significantly
458 overrepresented across DEGs and that have been previously related to the fermentation
459 process, including TFs belonging to the HAP complex. Moreover, our analysis also

460 highlighted the role of Cin5p as responsible for differences across strains. Cin5p is a basic
461 leucine zipper TF of the yAP-1 family, which participates in several stress conditions,
462 including oxidative and osmotic stress (54). While the HF knockout strains showed similar
463 phenotypes to those described in *S. cerevisiae*, i.e. lag phase lengthening in HAP complex
464 mutants (25), the QC18 strain showed a contrasting phenotype by significantly improving its
465 growth rate in the glucose-maltose shift in *hap4Δ*, *hap5Δ* and *cin5Δ* null mutants. In addition,
466 we demonstrated that *CIN5* allelic variants affect the growth rate and lag phase during the
467 diauxic shift, although no such differences were detected in fermentation, and mild
468 differences were observed for maltose consumption. Transcriptional regulation during the
469 diauxic shift in QC18 might be more complex than observed in other strains, and further
470 studies are needed to elucidate the role of these genes and allelic variants during this
471 transition.

472 In conclusion, the identification of natural allelic variants for fermentation rate is
473 instrumental to develop novel strains for brewing. In this study, we identified three TFs,
474 *HAP4*, *HAP5* and *CIN5,* that are responsible for differences in the glucose-maltose diauxic
475 shift between strains, with the most profound effect being present in *CIN5* allelic variants. In
476 this context, HF and LF strains exhibited unique gene expression patterns during
477 fermentation, with HF strains showing greater expression levels of maltose genes, while the
478 LF strains of glucose-related transporters. These differences could originate on the tree-host
479 from which this strain was isolated, which might determine the sugar source preference.
480 Novel alleles providing high fermentation rates will be of great value for the generation of
481 novel lager hybrids in the brewing industry.

MATERIALS AND METHODS

Strains and culture media

The *S. eubayanus* strains used in this work are listed in **Table S1A** and were collected from different Chilean and Argentinean localities (4–6). We also used the *S. pastorianus Saflager* W34/70 strain (Fermentis, France) as a lager fermentation control. All the strains were maintained on YPD solid media (1% yeast extract, 2% peptone, 2% glucose, 2 % agar). For long-term storage, the strains were maintained at -80 °C in 20% glycerol.

Fermentations in beer wort

Fermentations were carried out in three biological replicates as previously described (30). Briefly, 12 ºPlato (ºP) beer wort was oxygenated (15 mg L^{-1}) and supplemented with 0.3 ppm Zn^{2+} (as $ZnCl_2$). The pre-cultures were grown in 5 mL of 6 ºP wort for 24 h at 20 ºC in constant agitation at 150 rpm. Then, the inoculum was transferred to 50 mL 12 ºP wort and incubated for 24 h at 20 ºC in constant agitation at 150 rpm. The cells were collected by centrifugation at 5,000 x g for 5 min. The final cell concentration for each fermentation was estimated according to the formula described by (55). Cells were inoculated into 100 mL 12 ºP wort, using 250 mL bottles and airlocks with 30% glycerol. The fermentations were incubated at 12 ºC, with no agitation for 10-15 days, and monitored by weighing the bottles daily to determine weight loss over time. The maximum CO_2 loss rate (Vmax) was estimated using the R software version 4.1.1. The CO_2 loss curves were smoothened and the first derivative was plotted using the smooth.spline function. The maximum CO_2 loss rate coincides with the maximum point of the first derivative.

Metabolite quantification by HPLC

Sugar (glucose, fructose, maltose and maltotriose) and nitrogen (ammonium and amino acids) consumption, together with glycerol and ethanol production were determined by High-Performance Liquid Chromatography (HPLC) at different time-points during the fermentation process as previously described (8, 39, 56). These analyses were carried out in triplicate at 24 h, 48 h and on the final day of fermentation, and the consumption of each nitrogen source was estimated as the difference between the initial value and that of each time-point of the fermentation.

RNA-seq analysis

Gene expression analysis was performed on strains CL467.1, CBS12357 and QC18, which exhibited significant differences for different fermentative phenotypes. These strains were fermented in triplicate as previously described for 24 h. Then, cells were collected by centrifugation at 5,000 x g for 5 min and treated with two units of Zymolyase (Seikagaku Corporation, Japan) for 30 min at 37 ºC. RNA was extracted using the E.Z.N.A Total RNA Kit I (OMEGA) according to the manufacturer's instructions and treated with DNAse I (Promega) to remove genomic DNA traces. Total RNA was recovered using the GeneJET RNA Cleanup and Concentration Micro Kit (Thermo Fisher Scientific). RNA integrity was confirmed using a Fragment Analyzer (Agilent). RNA library preparation and Illumina sequencing were performed in the BGI facilities (Hong Kong, China) as previously described (30).

The quality of the raw reads was evaluated using the fastqc (https://www.bioinformatics.babraham.ac.uk/projects/fastqc/) tool. Reads were processed

using fastp (-3 l 40) (Chen et al., 2018) and mapped against the *S. eubayanus* CBS12357 reference genome (57) using STAR (58). Differentially expressed gene (DEG) analysis was performed using the DESeq2 package (59) in R v4.1.2, comparing the three strains at the same time. Genes with an adjusted *p-value* < 0.01 and an absolute value of fold change > 2 were considered DEGs for each comparison (CL467.1 vs. QC18, CBS12357 vs. QC18 and CL467.1 vs. CBS12357).

ATAC-seq data analysis

The assay for transposase accessible chromatin analysis (ATAC-seq) was performed on strains CL467.1, CBS12357 and QC18. These strains were fermented in duplicate and after 20 h and 72 h, 2.5 million cells were collected by centrifugation at 1,800 x g for 4 min at room temperature and washed twice using SB buffer (1 M sorbitol, 10 mM $MgCl_2$, 40 mM HEPES ph 7.5). Then, cells were treated with 50 mg/mL zymolyase 20T (Seikagaku Corporation, Japan) in SB buffer for 30 min at 30 °C. After incubation, cells were washed twice with SB buffer, resuspended in 50 µL transposition mix, containing 25 µL Nextera Tagment DNA buffer (Illumina, USA), 22.5 µL H_2O and 2.5 µL Nextera Tagment DNA enzyme I (Illumina, USA). After incubation for 30 min at 37 °C, DNA was purified using the DNA Clean and Concentrator-5 kit (Zymo Research), according to the manufacturer's instructions. Tagmented DNA was amplified by PCR using 1x NEBNext Hi-Fidelity PCR Master Mix (New England Biolabs, NEB), using Nextera Index i5 and i7 series PCR primers, and 5 µL tagmented DNA. Then, 50 µL of the amplified ATAC-seq library was subjected to double-sided size selection using magnetic beads (AMPure XP, Beckman Coulter). DNA bound to the beads was washed twice with 80% ethanol and then eluted in 20 µL H_2O. Library quality was assessed using a Fragment Analyzer (Agilent, USA) and quantified in Qubit

(Thermofisher, USA). Sequencing was conducted on a Nextseq 500 (Illumina, USA) in the Genomics unit at Universidad de Santiago de Chile. ATAC-seq reads were analyzed as previously described (56).

To match genes with their nearby ATAC-seq signal, we selected a regulatory region of 400 bp upstream of the start codon site for each gene. The ATAC-seq signals of 5,433 regulatory regions were quantified by counting mapped reads using featureCounts. Differential responses in ATAC-seq were estimated using DESeq2 (design= ~ condition).

Transcription factor binding scores (TFBSs) were calculated using TOBIAS (60) and the ScoreBigWig tool (--fp-min 5 --fp-max 30) for 141 yeast TFs from the JASPAR database (61). Binding scores were further processed in R. To calculate statistical differences in TFBSs, we employed a linear model using the limma R package (62). We considered binding differences with a FDR < 0.1 as statistically significant.

Gene Ontology (GO) analysis

GO analysis was performed using the tools provided by the DAVID Bioinformatics Resource (63, 64) using DEGs with *p-value* < 0.01 and absolute fold change values > 2. We selected categories with a significant over-representation utilizing a FDR < 10%.

Transcription factor analysis

Correlations between TFs and DEGs were predicted utilizing YeTFaSCo: Yeast Transcription Factor Specificity Compendium (32). Fold change values were used to test associations with potential regulators using a Spearman correlation.

The open reading frame (ORF) sequences of the selected TFs for strains CL467.1 and QC18 were obtained directly from the BAM files (.bam) mapped against the reference genome. BAM files were converted to VCF (Variant Calling Format) files using *freebayes*, which contained the genotype information of each gene and strain (65). Then, FASTA files were generated from VCF files using SAMtools (66). The nucleotide sequences were translated into amino acid sequences in Geneious v 8.1.8, utilizing the standard genetic code. Amino acids and nucleotide sequences were then aligned against the reference strain (CBS12357) using a Multiple Comparison by Log-Expectation (MUSCLE) algorithm with default parameters in Geneious v 8.1.8. The prediction of the change of each non-synonymous SNP over the protein sequence was analyzed using the online tool PROVEAN v1.1.3 (67).

Co-expression networks analyses

Co-expression networks were generated using a subset of the whole DEG set regulated by the TFs Hap4p, Hap5p, Cin5p and Put3p, as previously described (68). For this, we used read counts to calculate gene expression correlation. First, read counts were normalized to the number of reads that were effectively mapped, using the median normalization method available in the EBSeq R package (69). Subsequently, we added pseudocounts to avoid values equal to zero, generating a logarithmic matrix of the data. Finally, we used the Spearman correlation between each pair of selected groups of DEGs using the "psych" R package, retaining correlations with absolute values > 0.9 and adjusted *p-values* < 0.05. The network statistics, "degree" and "betweenness centrality", were calculated using "igraph" (https://igraph.org/). Cytoscape v 3.9.1(70) was used to visualize networks and corresponding statistics.

Generation of null mutants and reciprocal hemizygote strains

Null mutants for the *HAP5*, *HAP4*, *PUT3* and *CIN5* genes were generated using the CRISPR-Cas9 method (71) as previously described (9). Briefly, the gRNAs were designed using the Benchling online tool (https://www.benchling.com/) and cloned in the plasmid pAEF5 (a gift from Gilles Fischer, Addgene plasmid #136305) (72), using standard "Golden Gate Assembly" (73). CL467.1, CBS12357 and QC18 strains were co-transformed with the plasmid carrying the gRNA and the Cas9 gene, and with a synthetic double-stranded DNA fragment (donor DNA) composed of a 100 bp sequence containing flanking sequences of the target gene, corresponding to 50 bp upstream of start codon and 50 bp downstream of the stop codon. Correct gene deletion was confirmed by standard colony PCR. All the primers, gRNAs and donor DNA are listed in **Table S6**. Double null mutants for the TFs *HAP5* and *CIN5* were generated using the CRIPSR-Cas9 method as described above. The second null deletion was performed in *Δhap5* strains.

Reciprocal hemizygote strains were generated for *HAP5* and *CIN5* genes. The diploid wild type strains CL467.1, CBS12357, QC18 and their respective null mutant strains were sporulated on 2% potassium acetate agar plates (2% agar) for at least seven days at 12 °C. Meiotic segregants were obtained by dissecting tetrad ascospores treated with 10 µL Zymolyase 100T (50 mg/mL) in a SporePlay micromanipulator (Singer Instruments, UK) and crossed on YPD agar plates. Crossbreeding corresponds to crossing one wild type strain against another containing the mutated target gene. The plates were incubated at 25 °C for three days, then colonies were isolated and checked for the correct genotype by colony PCR. All the strains generated are listed in **Table S1B**.

Phenotypic characterization of strains

Wild type strains, null mutants and reciprocal hemizygote strains were phenotypically characterized under fermentation and/or microculture conditions as previously described (9, 30). Diauxic shift experiments were performed as previously published (30). Briefly, pre-cultures were grown in YP (1% yeast extract, 2% peptone) containing 5% glucose medium at 25 °C for 24 h. Cultures were diluted to an initial OD_{600nm} of 0.1 in fresh YP 5% glucose medium for an extra growth overnight. The next day, cultures were used to inoculate a 96-well plate with a final volume of 200 µL YP with the carbon source (5% glucose, 5% maltose, 5% galactose or 5% sucrose) at an initial OD_{600nm} of 0.1. The growth curves were monitored by measuring OD_{600nm} every 30 min in a TECAN Sunrise instrument. Lag phase and μ_{max} were estimated as previously described (25) using the R software version 4.1.2.

Data and statistical analyses

Statistical analysis and data visualization were performed using the R software version 4.1.2. The fermentation and growth kinetic parameters were compared using an analysis of variance (ANOVA) and the mean values of the three replicates were statistically analyzed with a Student's t-test and corrected for multiple comparisons using the Benjamini-Hochberg method. A *p-value* less than 0.05 ($p < 0.05$) was considered statistically significant. A principal component analysis (PCA) was performed using the FactoMineR package version 2.4 to compute principal component methods and the factoextra package version 1.07 for extracting, visualizing and interpreting the results. Heatmaps were generated using the ComplexHeatmap package version 2.6.2.

Data Accessibility

All sequences from RNA-seq and ATAC-seq have been deposited in the National Center for Biotechnology Information (NCBI) as a Sequence Read Archive under the BioProject accession number PRJNA857309.

ACKNOWLEDGMENTS

We thank Kamila Urbina, Antonio Molina and Jaime Ortega for their technical help, and Michael Handford (Universidad de Chile) for language support. FC acknowledges the Comisión Nacional de Investigación Científica y Tecnológica CONICYT FONDECYT [1220026] and ANID - Programa Iniciativa Científica Milenio - ICN17_022 and NCN2021_050. JM is supported by FONDECYT POSTDOCTORADO grant N° 3200545 and PV by FONDECYT POSTDOCTORADO grant N° 3200575. RN is supported by FIC "Transferencia Levaduras Nativas para Cerveza Artesanal" and FONDECYT grant N° 1180917. JBP is supported by Proyecto Dicyt Postdoc/ayudante 022243CR_Postdoc, Vicerrectoría de Investigación, Desarrollo e Innovación. DL is supported by CONICET project PIP 11220200102948CO; ANPCyT project PICT 2020-00226 and Universidad Nacional de Comahue. This research was partially supported by the supercomputing infrastructure of the National Laboratory for High Performance Computing Chile (NLHPC, ECM-02). We also acknowledge Fundación Ciencia & Vida for providing infrastructure, laboratory space and equipment for experiments. The funders had no role in study design, data collection and interpretation, or the decision to submit the work for publication.

References

1. Steensels J, Gallone B, Voordeckers K, Verstrepen KJ. 2019. Domestication of Industrial Microbes. Curr Biol 29:R381–R393.

656 2. Mozzachiodi S, Krogerus K, Gibson B, Nicolas A, Liti G. 2022. Unlocking the
657 functional potential of polyploid yeasts. Nat Commun 13:2580.

658 3. Libkind D, Hittinger CT, Valerio E, Goncalves C, Dover J, Johnston M, Goncalves P,
659 Sampaio JP. 2011. Microbe domestication and the identification of the wild genetic
660 stock of lager-brewing yeast. Proc Natl Acad Sci 108:14539–14544.

661 4. Nespolo RF, Villarroel CA, Oporto CI, Tapia SM, Vega-Macaya F, Urbina K, De
662 Chiara M, Mozzachiodi S, Mikhalev E, Thompson D, Larrondo LF, Saenz-Agudelo
663 P, Liti G, Cubillos FA. 2020. An Out-of-Patagonia migration explains the worldwide
664 diversity and distribution of Saccharomyces eubayanus lineages. PLoS Genet
665 16:e1008777.

666 5. Langdon QK, Peris D, Eizaguirre JI, Opulente DA, Buh K V., Sylvester K, Jarzyna
667 M, Rodríguez ME, Lopes CA, Libkind D, Hittinger CT. 2020. Postglacial migration
668 shaped the genomic diversity and global distribution of the wild ancestor of lager-
669 brewing hybrids. PLOS Genet 16:e1008680.

670 6. Eizaguirre JI, Peris D, Rodríguez ME, Lopes CA, De Los Ríos P, Hittinger CT,
671 Libkind D. 2018. Phylogeography of the wild Lager-brewing ancestor
672 (Saccharomyces eubayanus) in Patagonia. Environ Microbiol 20:3732–3743.

673 7. Villarreal P, Quintrel PA, Olivares-Muñoz S, Ruiz JI, Nespolo RF, Cubillos FA. 2021.
674 Identification of new ethanol-tolerant yeast strains with fermentation potential from
675 central Patagonia. Yeast yea.3662.

676 8. Mardones W, Villarroel CA, Krogerus K, Tapia SM, Urbina K, Oporto CI, Donnell

677 SO, Minebois R, Nespolo R, Fischer G, Querol A, Gibson B, Cubillos FA. 2020.
678 Molecular profiling of beer wort fermentation diversity across natural Saccharomyces
679 eubayanus isolates. Microb Biotechnol 1–14.

680 9. Molinet J, Urbina K, Villegas C, Abarca V, Oporto CI, Villarreal P, Villarroel CA,
681 Salinas F, Nespolo RF, Cubillos FA. 2022. A Saccharomyces eubayanus haploid
682 resource for research studies. Sci Rep 12.

683 10. Burini JA, Eizaguirre JI, Loviso C, Libkind D. 2022. Selection of Saccharomyces
684 eubayanus strains from Patagonia (Argentina) with brewing potential and performance
685 in the craft beer industry. Eur Food Res Technol 248:519–531.

686 11. Gallone B, Steensels J, Mertens S, Dzialo MC, Gordon JL, Wauters R, Theßeling FA,
687 Bellinazzo F, Saels V, Herrera-Malaver B, Prahl T, White C, Hutzler M, Meußdoerffer
688 F, Malcorps P, Souffriau B, Daenen L, Baele G, Maere S, Verstrepen KJ. 2019.
689 Interspecific hybridization facilitates niche adaptation in beer yeast. Nat Ecol Evol
690 3:1562–1575.

691 12. Langdon QK, Peris D, Baker ECP, Opulente DA, Nguyen HV, Bond U, Gonçalves P,
692 Sampaio JP, Libkind D, Hittinger CT. 2019. Fermentation innovation through
693 complex hybridization of wild and domesticated yeasts. Nat Ecol Evol 3:1576–1586.

694 13. Almeida P, Gonçalves C, Teixeira S, Libkind D, Bontrager M, Masneuf-Pomarède I,
695 Albertin W, Durrens P, Sherman DJ, Marullo P, Todd Hittinger C, Gonçalves P,
696 Sampaio JP. 2014. A Gondwanan imprint on global diversity and domestication of
697 wine and cider yeast Saccharomyces uvarum. Nat Commun 5.

698 14. Baker ECP, Peris D, Moriarty R V., Li XC, Fay JC, Hittinger CT. 2019. Mitochondrial
699 DNA and temperature tolerance in lager yeasts. Sci Adv 5:1–8.

700 15. Krogerus K, Arvas M, De Chiara M, Magalhães F, Mattinen L, Oja M, Vidgren V,
701 Yue JX, Liti G, Gibson B. 2016. Ploidy influences the functional attributes of de novo
702 lager yeast hybrids. Appl Microbiol Biotechnol 100:7203–7222.

703 16. Gorter De Vries AR, Pronk JT, Daran JMG. 2019. Lager-brewing yeasts in the era of
704 modern genetics. FEMS Yeast Res 19:1–17.

705 17. Peris D, Sylvester K, Libkind D, Gonçalves P, Sampaio JP, Alexander WG, Hittinger
706 CT. 2014. Population structure and reticulate evolution of Saccharomyces eubayanus
707 and its lager-brewing hybrids. Mol Ecol 23:2031–2045.

708 18. Peris D, Langdon QK, Moriarty R V., Sylvester K, Bontrager M, Charron G, Leducq
709 JB, Landry CR, Libkind D, Hittinger CT. 2016. Complex Ancestries of Lager-
710 Brewing Hybrids Were Shaped by Standing Variation in the Wild Yeast
711 Saccharomyces eubayanus. PLoS Genet 12:1–20.

712 19. Bing J, Han PJ, Liu WQ, Wang QM, Bai FY. 2014. Evidence for a far east asian origin
713 of lager beer yeast. Curr Biol 24:R380–R381.

714 20. Gayevskiy V, Goddard MR. 2016. Saccharomyces eubayanus and Saccharomyces
715 arboricola reside in North Island native New Zealand forests. Environ Microbiol
716 18:1137–1147.

717 21. Brickwedde A, van den Broek M, Geertman JMA, Magalhães F, Kuijpers NGA,

718 Gibson B, Pronk JT, Daran JMG. 2017. Evolutionary engineering in chemostat
719 cultures for improved maltotriose fermentation kinetics in saccharomyces pastorianus
720 lager brewing yeast. Front Microbiol 8:1–15.

721 22. Krogerus K, Magalhães F, Vidgren V, Gibson B. 2017. Novel brewing yeast hybrids:
722 creation and application. Appl Microbiol Biotechnol 101:65–78.

723 23. Cubillos FA, Gibson B, Grijalva-Vallejos N, Krogerus K, Nikulin J. 2019.
724 Bioprospecting for brewers: Exploiting natural diversity for naturally diverse beers.
725 Yeast https://doi.org/10.1002/yea.3380.

726 24. Albergaria H, Arneborg N. 2016. Dominance of Saccharomyces cerevisiae in
727 alcoholic fermentation processes: role of physiological fitness and microbial
728 interactions. Appl Microbiol Biotechnol 100:2035–2046.

729 25. Perez-Samper G, Cerulus B, Jariani A, Vermeersch L, Barrajón Simancas N,
730 Bisschops MMM, van den Brink J, Solis-Escalante D, Gallone B, De Maeyer D, van
731 Bael E, Wenseleers T, Michiels J, Marchal K, Daran-Lapujade P, Verstrepen KJ. 2018.
732 The Crabtree Effect Shapes the Saccharomyces cerevisiae Lag Phase during the
733 Switch between Different Carbon Sources. MBio 9:1–18.

734 26. Nikulin J, Krogerus K, Gibson B. 2018. Alternative Saccharomyces interspecies
735 hybrid combinations and their potential for low-temperature wort fermentation. Yeast
736 35:113–127.

737 27. Nikulin J, Vidgren V, Krogerus K, Magalhães F, Valkeemäki S, Kangas-Heiska T,
738 Gibson B. 2020. Brewing potential of the wild yeast species Saccharomyces

paradoxus. Eur Food Res Technol 246:2283–2297.

28. Hutzler M, Michel M, Kunz O, Kuusisto T, Magalhães F, Krogerus K, Gibson B. 2021. Unique Brewing-Relevant Properties of a Strain of Saccharomyces jurei Isolated From Ash (Fraxinus excelsior). Front Microbiol 12:1–14.

29. Kayikci Ö, Nielsen J. 2015. Glucose repression in Saccharomyces cerevisiae. FEMS Yeast Res 15:1–8.

30. Mardones W, Villarroel CA, Abarca V, Urbina K, Peña TA, Molinet J, Nespolo RF, Cubillos FA. 2021. Rapid selection response to ethanol in Saccharomyces eubayanus emulates the domestication process under brewing conditions. Microb Biotechnol 2:1–18.

31. Burini JA, Eizaguirre JI, Loviso C, Libkind D. 2021. Non-conventional yeasts as tools for innovation and differentiation in brewing. Rev Argent Microbiol https://doi.org/10.1016/j.ram.2021.01.003.

32. De Boer CG, Hughes TR. 2012. YeTFaSCo: A database of evaluated yeast transcription factor sequence specificities. Nucleic Acids Res 40:169–179.

33. Mao Y, Chen C. 2019. The Hap Complex in Yeasts: Structure, Assembly Mode, and Gene Regulation. Front Microbiol 10.

34. Rodrigues-Pousada C, Devaux F, Caetano SM, Pimentel C, da Silva S, Cordeiro AC, Amaral C. 2019. Yeast AP-1 like transcription factors (Yap) and stress response: A current overview. Microb Cell 6:267–285.

759 35. Mat Nanyan NS binti, Takagi H. 2020. Proline Homeostasis in Saccharomyces
760 cerevisiae: How Does the Stress-Responsive Transcription Factor Msn2 Play a Role?
761 Front Genet 11:1–9.

762 36. Fujita A, Hiroko T, Hiroko F, Oka C. 2005. Enhancement of superficial pseudohyphal
763 growth by overexpression of the SFG1 gene in yeast Saccharomyces cerevisiae. Gene
764 363:97–104.

765 37. Contreras-Shannon V, Lin AP, McCammon MT, McAlister-Henn L. 2005. Kinetic
766 properties and metabolic contributions of yeast mitochondrial and cytosolic NADP+-
767 specific isocitrate dehydrogenases. J Biol Chem 280:4469–4475.

768 38. Oomuro M, Watanabe D, Sugimoto Y, Kato T, Motoyama Y, Watanabe T, Takagi H.
769 2018. Accumulation of intracellular S-adenosylmethionine increases the fermentation
770 rate of bottom-fermenting brewer's yeast during high-gravity brewing. J Biosci
771 Bioeng 126:736–741.

772 39. Urbina K, Villarreal P, Nespolo RF, Salazar R, Santander R, Cubillos FA. 2020.
773 Volatile compound screening using HS-SPME-GC/MS on saccharomyces eubayanus
774 strains under low-temperature pilsner wort fermentation. Microorganisms 8:1–19.

775 40. Ciani M, Capece A, Comitini F, Canonico L, Siesto G, Romano P. 2016. Yeast
776 interactions in inoculated wine fermentation. Front Microbiol 7:1–7.

777 41. Eliodório KP, Cunha GC de G e., Müller C, Lucaroni AC, Giudici R, Walker GM,
778 Alves SL, Basso TO. 2019. Advances in yeast alcoholic fermentations for the
779 production of bioethanol, beer and wine, p. 61–119. *In* Advances in Applied

780 Microbiology.

781 42. Berthels NJ, Cordero Otero RR, Bauer FF, Thevelein JM, Pretorius IS. 2004.
782 Discrepancy in glucose and fructose utilisation during fermentation by Saccharomyces
783 cerevisiae wine yeast strains. FEMS Yeast Res 4:683–689.

784 43. Magalhães F, Vidgren V, Ruohonen L, Gibson B. 2016. Maltose and maltotriose
785 utilisation by group I strains of the hybrid lager yeast Saccharomyces pastorianus.
786 FEMS Yeast Res 16:1–11.

787 44. Kremer A. 2016. Microevolution of European temperate oaks in response to
788 environmental changes. C R Biol 339:263–267.

789 45. Salas-Eljatib C. 2021. An approach to quantify climate–productivity relationships: an
790 example from a widespread Nothofagus forest. Ecol Appl 31:1–14.

791 46. Ferreira JPA, Miranda I, Sousa VB, Pereira H. 2018. Chemical composition of barks
792 from Quercus faginea trees and characterization of their lipophilic and polar extracts.
793 PLoS One 13:1–18.

794 47. Fajardo A, McIntire EJB. 2010. Merged trees in second-growth, fire-origin forests in
795 Patagonia, Chile: positive spatial association patterns and their ecological
796 implications. Am J Bot 97:1424–1430.

797 48. Cerulus B, Jariani A, Perez-Samper G, Vermeersch L, Pietsch JMJ, Crane MM, New
798 AM, Gallone B, Roncoroni M, Dzialo MC, Govers SK, Hendrickx JO, Galle E,
799 Coomans M, Berden P, Verbandt S, Swain PS, Verstrepen KJ. 2018. Transition

between fermentation and respiration determines history-dependent behavior in fluctuating carbon sources. Elife 7.

49. New AM, Cerulus B, Govers SK, Perez-Samper G, Zhu B, Boogmans S, Xavier JB, Verstrepen KJ. 2014. Different Levels of Catabolite Repression Optimize Growth in Stable and Variable Environments. PLoS Biol 12:17–20.

50. Gibson BR, Boulton CA, Box WG, Graham NS, Lawrence SJ, Linforth RST, Smart KA. 2008. Carbohydrate utilization and the lager yeast transcriptome during brewery fermentation. Yeast 25:549–562.

51. Diderich JA, Schuurmans JM, Van Gaalen MC, Kruckeberg AL, Van Dam K. 2001. Functional analysis of the hexose transporter homologue HXT5 in Saccharomyces cerevisiae. Yeast 18:1515–1524.

52. Horák J. 2013. Regulations of sugar transporters: insights from yeast. Curr Genet 59:1–31.

53. Broach JR. 2012. Nutritional Control of Growth and Development in Yeast. Genetics 192:73–105.

54. Rodrigues-Pousada C, Menezes RA, Pimentel C. 2010. The Yap family and its role in stress response. Yeast 27:245–258.

55. White C, Zainasheff J. 2010. Yeast: The Practical Guide to Beer Fermentation. Brewers Publications.

56. Villarroel CA, Bastías M, Canessa P, Cubillos FA. 2021. Uncovering Divergence in

Gene Expression Regulation in the Adaptation of Yeast to Nitrogen Scarcity. mSystems 6.

57. Brickwedde A, Brouwers N, Broek M van den, Gallego Murillo JS, Fraiture JL, Pronk JT, Daran JMG. 2018. Structural, physiological and regulatory analysis of maltose transporter genes in Saccharomyces eubayanus CBS 12357T. Front Microbiol 9:1–18.

58. Dobin A, Davis CA, Schlesinger F, Drenkow J, Zaleski C, Jha S, Batut P, Chaisson M, Gingeras TR. 2013. STAR: Ultrafast universal RNA-seq aligner. Bioinformatics 29:15–21.

59. Love MI, Huber W, Anders S. 2014. Moderated estimation of fold change and dispersion for RNA-seq data with DESeq2. Genome Biol 15:1–21.

60. Bentsen M, Goymann P, Schultheis H, Klee K, Petrova A, Wiegandt R, Fust A, Preussner J, Kuenne C, Braun T, Kim J, Looso M. 2020. ATAC-seq footprinting unravels kinetics of transcription factor binding during zygotic genome activation. Nat Commun 11.

61. Fornes O, Castro-Mondragon JA, Khan A, Van Der Lee R, Zhang X, Richmond PA, Modi BP, Correard S, Gheorghe M, Baranašić D, Santana-Garcia W, Tan G, Chèneby J, Ballester B, Parcy F, Sandelin A, Lenhard B, Wasserman WW, Mathelier A. 2020. JASPAR 2020: Update of the open-Access database of transcription factor binding profiles. Nucleic Acids Res 48:D87–D92.

62. Ritchie ME, Phipson B, Wu D, Hu Y, Law CW, Shi W, Smyth GK. 2015. Limma powers differential expression analyses for RNA-sequencing and microarray studies.

Nucleic Acids Res 43:e47.

63. Huang DW, Sherman BT, Lempicki RA. 2009. Systematic and integrative analysis of large gene lists using DAVID bioinformatics resources. Nat Protoc 4:44–57.

64. Huang DW, Sherman BT, Lempicki RA. 2009. Bioinformatics enrichment tools: Paths toward the comprehensive functional analysis of large gene lists. Nucleic Acids Res 37:1–13.

65. Garrison E, Marth G. 2012. Haplotype-based variant detection from short-read sequencing. arXiv 1–9.

66. Li H, Handsaker B, Wysoker A, Fennell T, Ruan J, Homer N, Marth G, Abecasis G, Durbin R. 2009. The Sequence Alignment/Map format and SAMtools. Bioinformatics 25:2078–2079.

67. Choi Y, Chan AP. 2015. PROVEAN web server: A tool to predict the functional effect of amino acid substitutions and indels. Bioinformatics 31:2745–2747.

68. Contreras-López O, Moyano TC, Soto DC, Gutiérrez RA. 2018. Step-by-step construction of gene co-expression networks from high-throughput Arabidopsis RNA sequencing data. Methods Mol Biol 1761:275–301.

69. Leng N, Dawson JA, Thomson JA, Ruotti V, Rissman AI, Smits BMG, Haag JD, Gould MN, Stewart RM, Kendziorski C. 2013. Gene expression EBSeq : an empirical Bayes hierarchical model for inference in RNA-seq experiments. Bioinformatics 29:1035–1043.

70. Shannon P, Markiel A, Ozier O, Baliga NS, Wang JT, Ramage D, Amin N, Schwikowski B, Ideker T. 2003. Cytoscape: A Software Environment for Integrated Models of Biomolecular Interaction Networks. Genome Res 13:2498–2504.

71. Dicarlo JE, Norville JE, Mali P, Rios X, Aach J, Church GM. 2013. Genome engineering in Saccharomyces cerevisiae using CRISPR-Cas systems. Nucleic Acids Res 41:4336–4343.

72. Fleiss A, O'Donnell S, Fournier T, Lu W, Agier N, Delmas S, Schacherer J, Fischer G. 2019. Reshuffling yeast chromosomes with CRISPR/Cas9. PLOS Genet 15:e1008332.

73. Horwitz AA, Walter JM, Schubert MG, Kung SH, Hawkins K, Platt DM, Hernday AD, Mahatdejkul-Meadows T, Szeto W, Chandran SS, Newman JD. 2015. Efficient Multiplexed Integration of Synergistic Alleles and Metabolic Pathways in Yeasts via CRISPR-Cas. Cell Syst 1:88–96.

Author Contributions

J.M., J.I.E., D.L. and F.A.C.: conceptualization; J.M., J.I.E., P.Q., D.L. and F.A.C.: methodology; J.M., C.A.V., N.B. and P.V.: software; J.M., R.F.N., D.L. and F.A.C.: validation; J.M., P.Q., N.B. and C.A.V.: formal analysis; J.M., J.I.E., P.Q., P.V., J.B.-P. and C.A.V.: investigation; J.M., P.V., R.F.N., D.L. and F.A.C.: resources; J.M., P.Q. and C.A.V.: visualization; J.M., P.Q., C.A.V. and N.B.: data curation; J.M., J.I.E., C.A.V. and F.A.C.: writing-original draft preparation. All authors have read and agreed to the published version of the manuscript.

FIGURES

Figure 1. Fermentation differences between Andean Patagonia *S. eubayanus* strains. (A) Map of Argentinian/Chilean Andean Patagonia together with the eight localities from where the 19 strains were isolated. (B) CO_2 loss kinetics for 19 strains; red, blue and light blue depict the three strains selected for the rest of this study. (C) Principal component analysis (PCA) using fermentation parameters across the 19 strains, together with the distribution of individual strains. Arrows depict the different parameters. (D) Maltose consumption kinetics of CBS12357, CL467.1 and QC18 strains. Plotted values correspond to mean values of three independent replicates for each strain. The (*) represents different levels of significance between QC18 and the other strains (t-test, **** $p \leq 0.0001$).

Figure 2. Diauxic shift differences between LF and HF strains during the glucose-maltose shift. (A) Growth curves in glucose and the kinetic parameters: growth rate and lag time. (B) Growth curves in glucose-maltose shifts and the kinetic parameters relative to growth in glucose. (C) Growth curves in maltose and the kinetic parameters relative to the growth in glucose. Plotted values correspond to the mean value of three independent replicates for each strain. The (*) represents different levels of significance between QC18 (LF) and the other strains (CBS12357 and CL467.1, HF) (t-test, * $p \leq 0.05$, ** $p \leq 0$ .01, *** $p \leq 0.001$, **** $p \leq 0.0001$).

Figure 3. Comparative transcriptome analysis between HF and LF strains. (A) Venn diagram of differentially expressed genes (DEGs), and up and downregulated genes in CBS12357 (HF) vs. QC18 (LF), CL467.1 (HF) vs. QC18 and CL467.1 vs. CBS12357 strains. (B) Hierarchical clustering of DEGs in the three strains. The heatmap was generated using

the z-score of expression levels in each comparison. Each row represents a given gene and each column represents a different strain. Clusters are annotated at the right, together with their gene ontology (GO) category. (C) Network analysis of DEGs regulated by Hap4p, Put3p, Cin5p and Hap5 in strains with high fermentation capacity vs. QC18 strain, depicting in bold the most relevant hubs. Red and blue lines represent positive and negative correlations, respectively.

Figure 4. Differences in chromatin accessibility and transcription factor binding between HF and LF strains. (A) The heatmap shows a hierarchical clustering analysis of chromatin accessibility at promoter regions of HF (CBS12357 and CL467.1) and LF (QC18) strains 20 h after fermentation. Accessibility from ATAC-seq FPKM values were transformed to z-scores and normalized by row. Gene expression at 20 h is shown as log2 fold changes of CL467.1 and CBS12357 relative to QC18. (B) The Venn diagram shows the number of differentially accessible regions (DARs) and their intersection showing higher or lower accessibility in the HF and LF strains in the contrast between 72 and 20 h of fermentation. (C) Gene ontology (GO) enrichment analyses for DARs highlight higher accessibility after 72 h of fermentation. GO terms correspond to Biological Processes. (D) The heatmap shows transcription factor binding scores (TFBS) obtained from ATAC-seq TF binding footprints transformed to z-scores and normalized by row. Gene expression is shown as in (A).

Figure 5. Effect of Hap4p, Hap5, Cin5p and Put3p on diauxic shift and fermentation capacity. (A) Lag time and growth rate of null mutant strains relative to wild type strains after glucose-maltose shift. (B) Fermentation rate and maximum CO_2 loss of null mutant strains relative to wild type strains. (C) Maltose consumption and ethanol production kinetics

of CL467.1 and QC18 *cin5* null mutant strains. Plotted values correspond to the means of three independent replicates of each strain. The (*) represents different levels of significance between mutant and wild type strains (t-test, * $p \leq 0.05$, ** $p \leq 0.01$, *** $p \leq 0.001$, **** $p \leq 0.0001$).

SUPLEMENTAL MATERIAL

Figure S1. (A) Pearson correlation for residual maltose versus CO_2 loss rate, maximum CO_2 loss and ethanol production. (B) Pearson correlation for CO_2 loss rate versus Maximum CO_2 loss. (C) Hierarchically clustered heatmap of kinetic parameters. Phenotypic values are calculated as normalized z-scores.

Figure S2. (A) Growth curves obtained after glucose-galactose and glucose-sucrose shift. (B) Growth rates and (C) Lag times after glucose-galactose and glucose-sucrose shift.

Figure S3. (A) Principal components analysis of DEGs. (B) Transcription factor binding scores (TFBS) for Cin5p, Hap1, Hap2, Hap3, Hap5 and Put3 at 20 h and 72 h.

Figure S4. Effect of Hap4p, Hap5, Cin5p and Put4p on the growth in glucose (A), after glucose-galactose shift (B) and after glucose-sucrose shift (C). Reciprocal hemygosity analysis for *CIN5* gene on kinetic parameters after glucose-maltose shift in QC18 x CL467.1 and QC18 x CBS12357 strains (D).

Table S1. (A) *Saccharomyces eubayanus* strains used in this work. (B) Strains generated in this study.

946 **Table S2.** (A) Fermentation kinetic parameter. (B) Statistical analysis for maximum CO_2 loss
947 and CO_2 loss rate. (C) Residual sugar (g/L) and ethanol production (%v/v) at the end of the
948 fermentation. (D) Statistical analysis for residual sugar and ethanol production. (E) Residual
949 sugar (g/L) and ethanol production (%v/v) for QC18, CL467.1 and CBS12357 strains at 24,
950 48, 168 and 336 hours. (F) Residual nitrogen (mg N/L) at the end of the fermentation. (G)
951 Statistical analysis for nitrogen consumption. (H) Residual nitrogen (mg N/L) for QC18,
952 CL467.1 and CBS12357 strains at 24, 48 and 336 hours.

953 **Table S3**. Growth rates and lag times after diauxic shift.

954 **Table S4**. (A) Levels of genes expression in strains. (B) DEGs in the six clusters of
955 expression profiles. (C) GO analysis to cluster of expression profiles. (D) Transcriptional
956 factors (TF) regulating genes differentially expressed (absolute log2FC > 1) between
957 CBS12357 and QC18. (E) Transcriptional factors (TF) regulating genes differentially
958 expressed (absolute log2FC > 1) between CL467.1 and QC18. (F) Transcriptional factors
959 (TF) regulating genes differentially expressed (absolute log2FC > 1) between CL467.1 and
960 CBS12357. (G) SNPs present in the four transcription factor respect to reference strain
961 CBS12357. (H) Amino acid substitution in the four transcription factor respect to reference
962 strain CBS12357. (I) Differentially accessible regions between HF and LF strains at 20 hours
963 of fermentation. (J) Differentially accessible regions between HF and LF strains at 72 hours
964 of fermentation.

965 **Table S5**. (A) Growth rates and Lag times after diauxic shift in mutant strains. (B) Growth
966 rates and Lag times after diauxic shift in reciprocal hemizygote strains. (C) Kinetic
967 parameters from fermentations of mutant strains. (D) Residual maltose (g/L) and ethanol

968 production (%v/v) for QC18 and CL467.1 *CIN5* null mutant strains at 24, 48, 120, 168 and

969 336 hours.

970 **Table S6**. Primers used in this study.

(A)

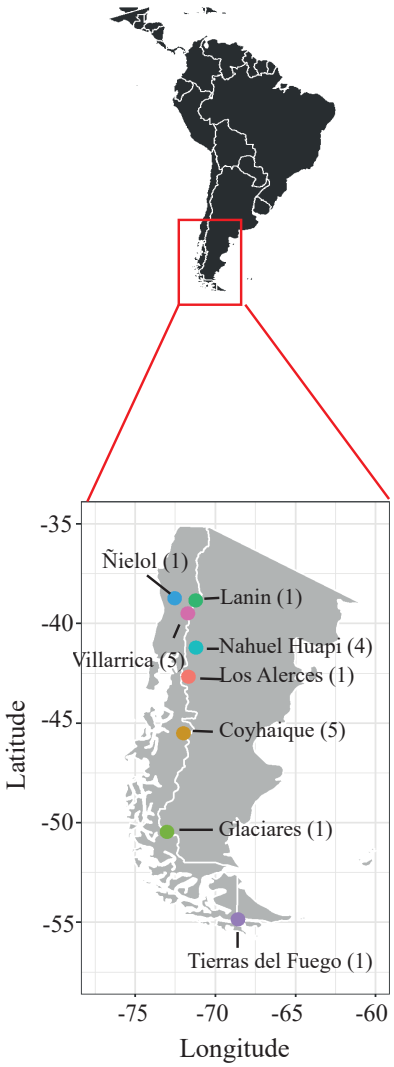
Ñielol (1)
Lanin (1)
Villarrica (5)
Nahuel Huapi (4)
Los Alerces (1)
Coyhaique (5)
Glaciares (1)
Tierras del Fuego (1)
Latitude
Longitude
-35
-40
-45
-50
-55
-75
-70
-65
-60

(B)

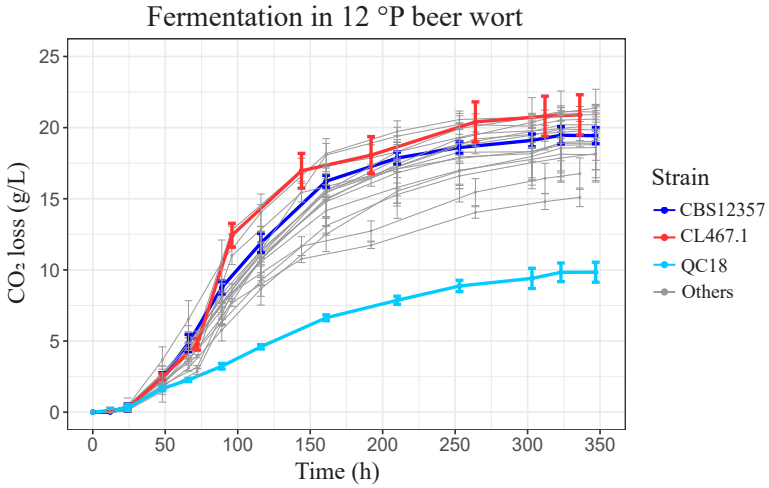
Fermentation in 12 °P beer wort
CO₂ loss (g/L)
Time (h)
Strain
CBS12357
CL467.1
QC18
Others

(C)

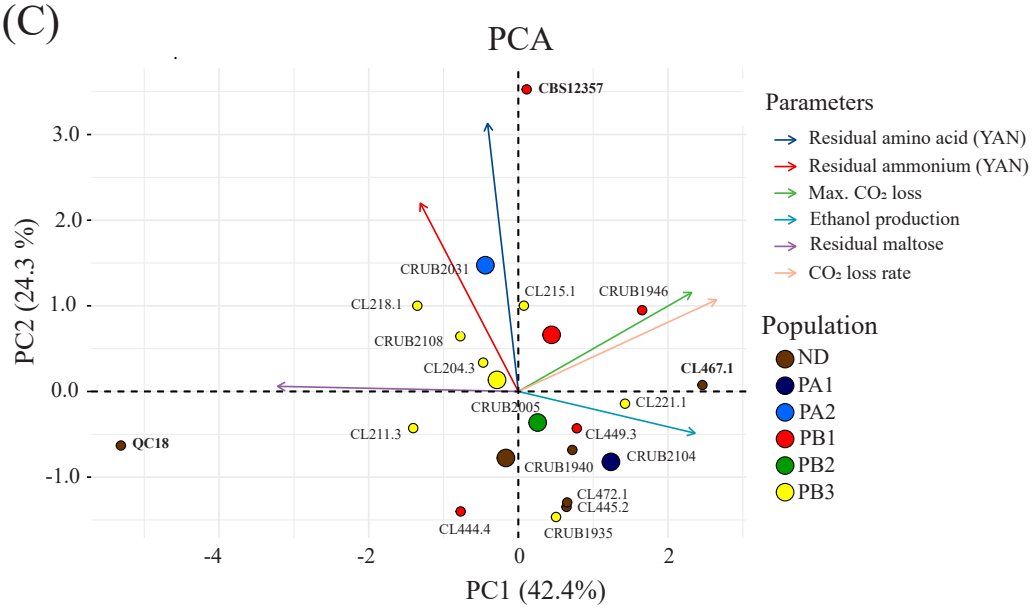
PCA
PC2 (24.3 %)
PC1 (42.4%)
CBS12357
CRUB2031
CL218.1
CRUB2108
CL204.3
CL215.1
CRUB1946
CL467.1
CRUB2005
CL221.1
CL211.3
CL449.3
QC18
CRUB1940
CRUB2104
CL472.1
CL445.2
CL444.4
CRUB1935
Parameters
Residual amino acid (YAN)
Residual ammonium (YAN)
Max. CO₂ loss
Ethanol production
Residual maltose
CO₂ loss rate
Population
ND
PA1
PA2
PB1
PB2
PB3

(D)

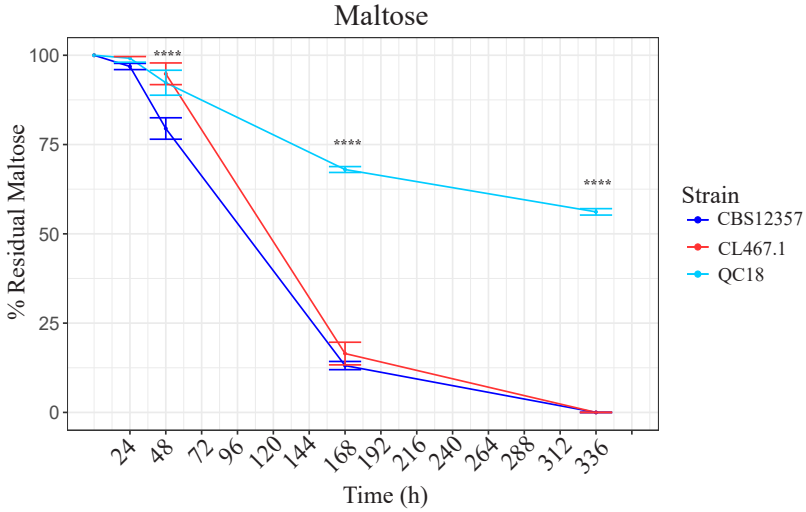
Maltose
% Residual Maltose
Time (h)
****
Strain
CBS12357
CL467.1
QC18

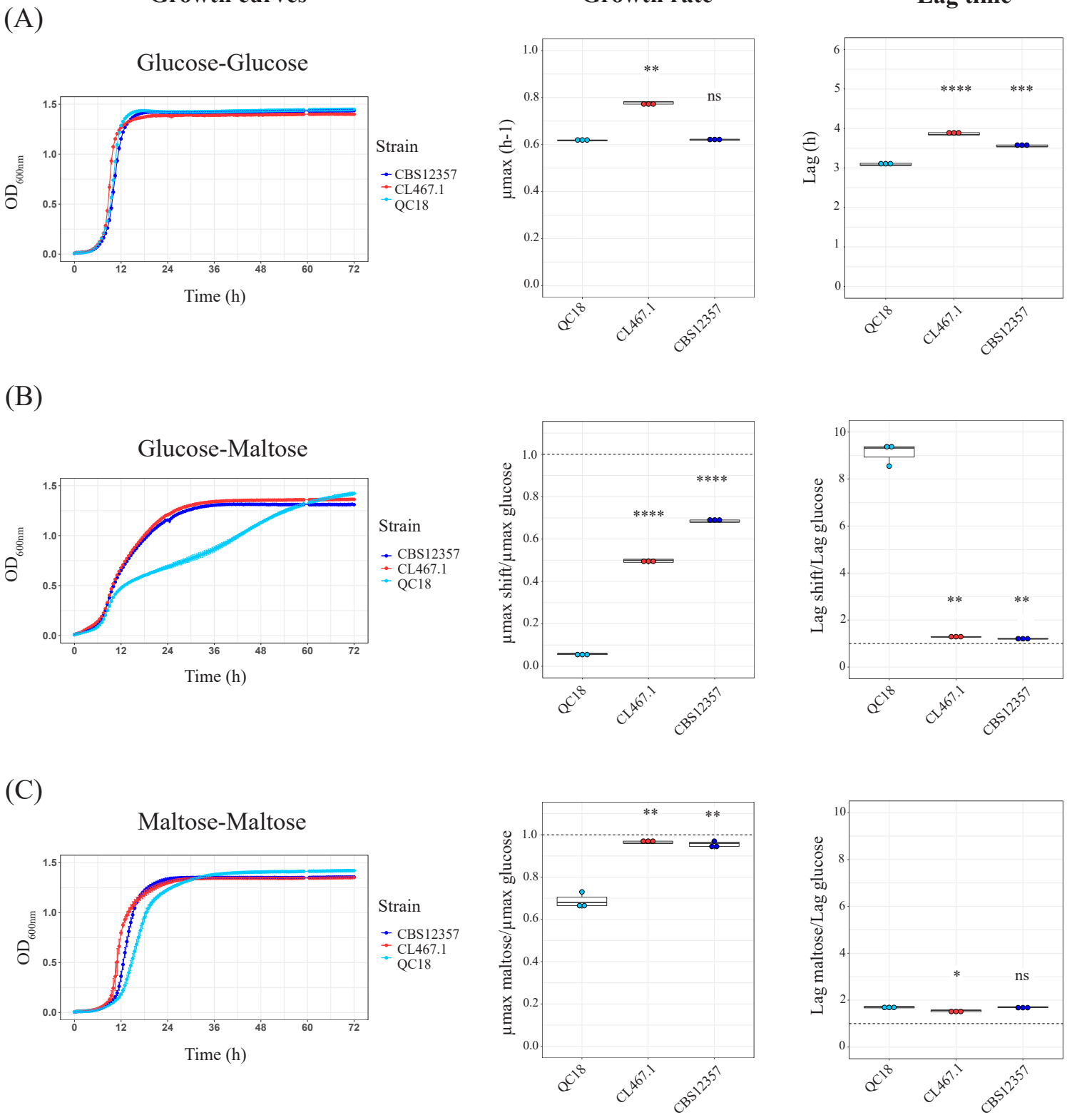
Growth curves
Growth rate
Lag time
(A)
Glucose-Glucose
OD600nm
Time (h)
Strain
CBS12357
CL467.1
QC18
μmax (h-1)
Lag (h)
**
ns
****
***
(B)
Glucose-Maltose
μmax shift/μmax glucose
Lag shift/Lag glucose
****
**
(C)
Maltose-Maltose
μmax maltose/μmax glucose
Lag maltose/Lag glucose
*

(A)

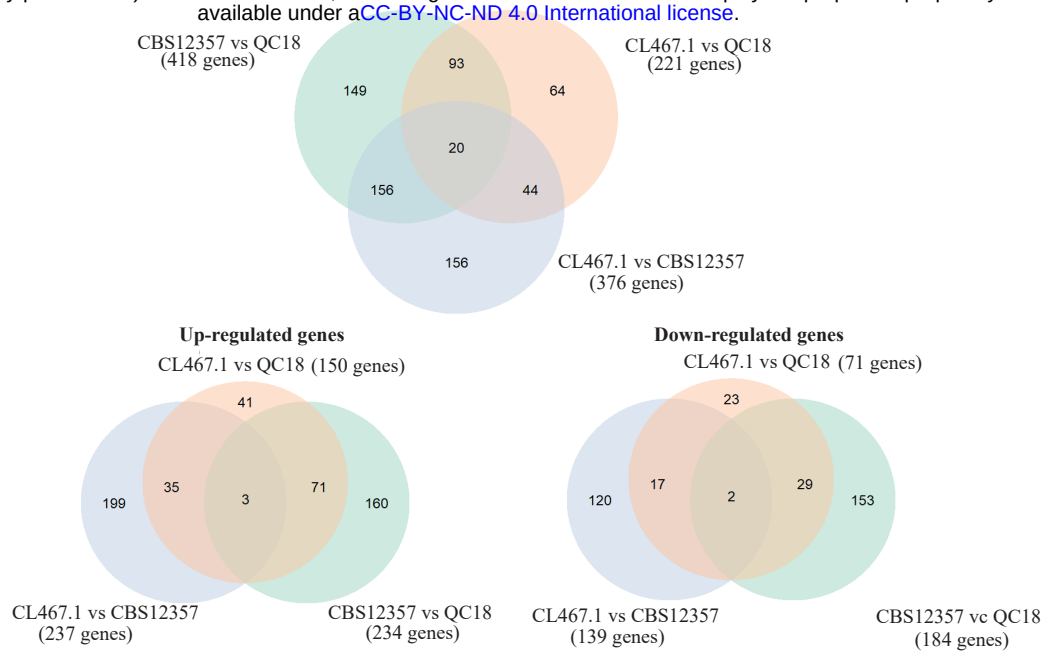

(B)

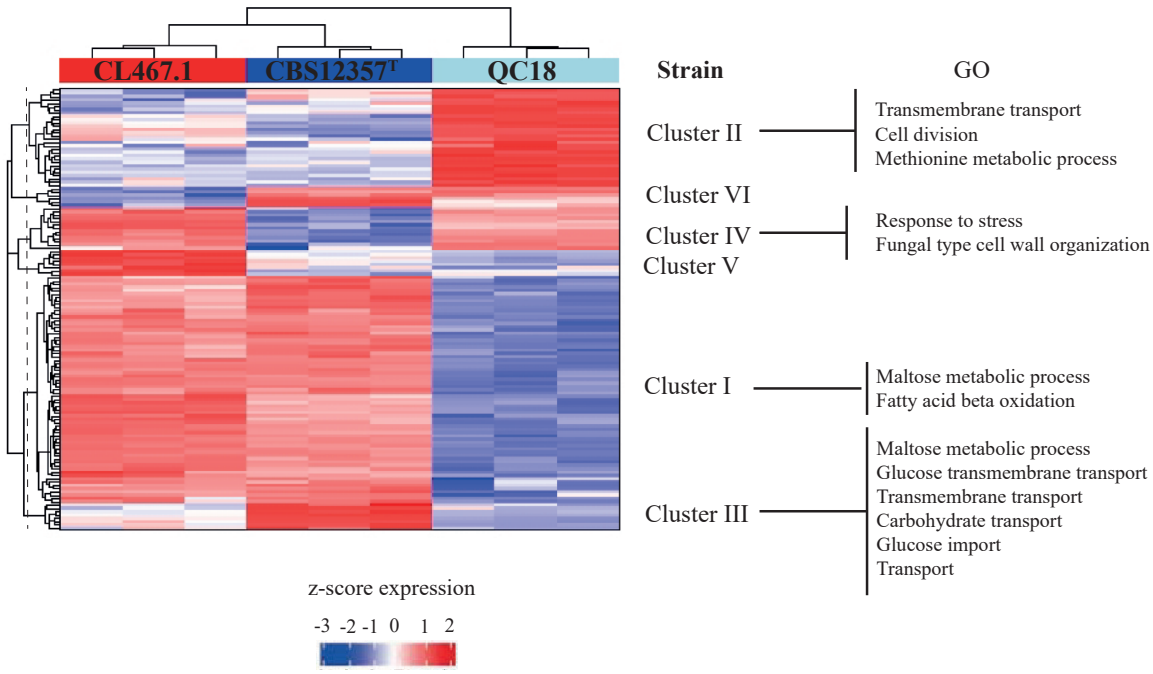

(C)

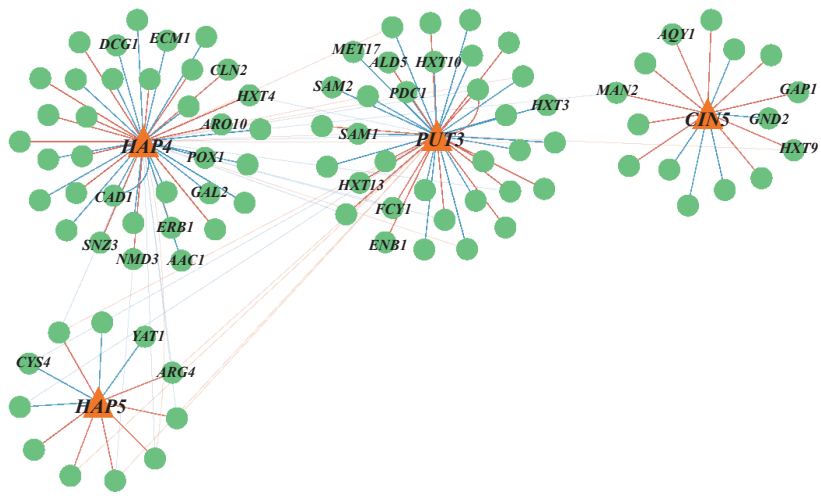

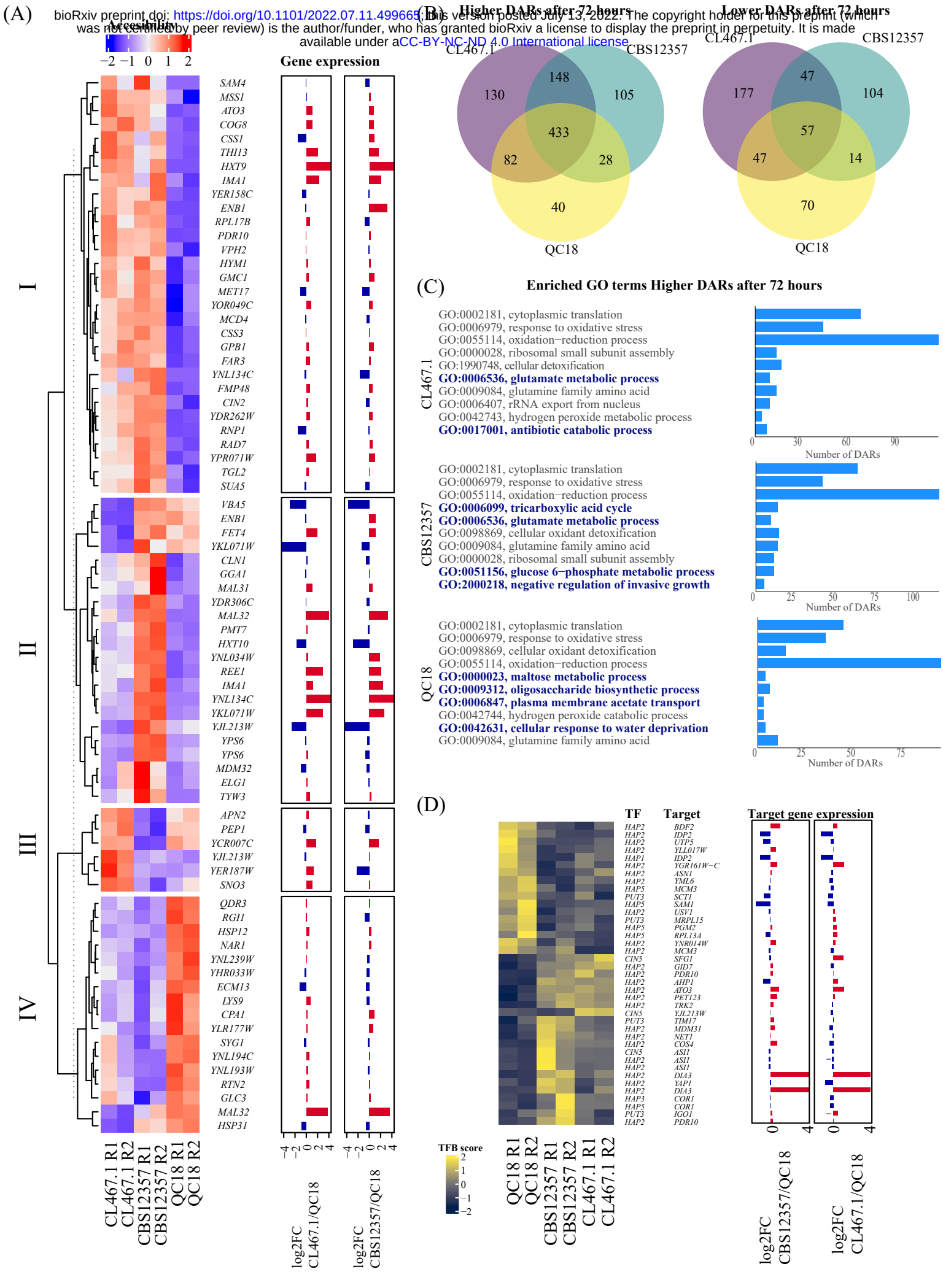

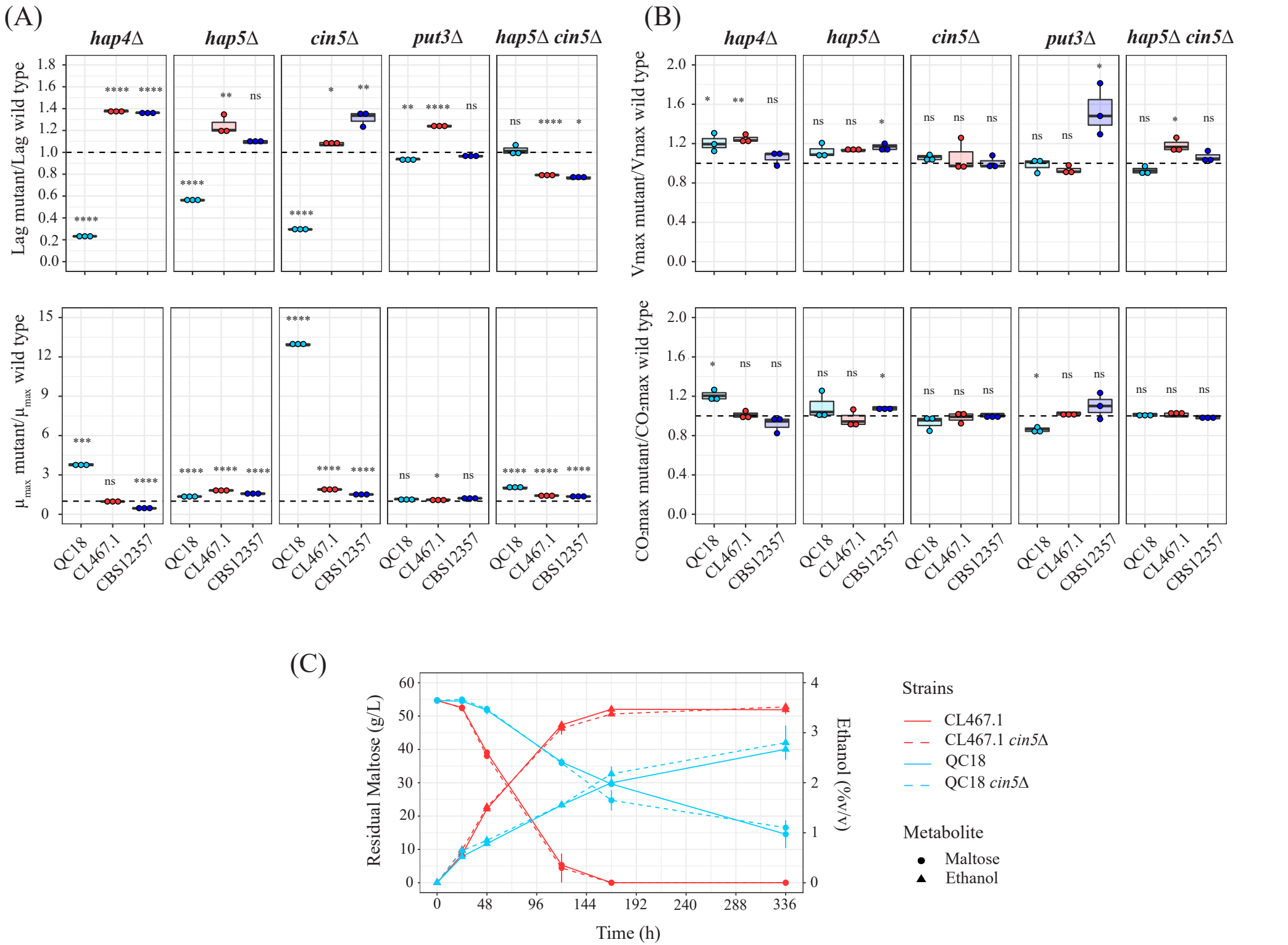
(A)
(B)
(C)
hap4Δ
hap5Δ
cin5Δ
put3Δ
hap5Δ cin5Δ
Lag mutant/Lag wild type
μmax mutant/μmax wild type
Vmax mutant/Vmax wild type
CO2max mutant/CO2max wild type
QC18
CL467.1
CBS12357
Residual Maltose (g/L)
Ethanol (%v/v)
Time (h)
Strains
CL467.1
CL467.1 cin5Δ
QC18
QC18 cin5Δ
Metabolite
Maltose
Ethanol